Ion effects on alkaline conjugation and acid stability of casein-propylene glycol alginate dispersions

A Thesis Presented for the

Master of Science

Degree

The University of Tennessee, Knoxville

Bryan Alberto Castellanos Paez

December 2024

ACKNOWLEDGEMENTS

I would like to extend my sincere appreciation to my major advisor Dr. Qixin Zhong. He is the most disciplined, hardworking, smart, and passionate person I have ever met in the professional field. This thesis is dedicated not only to my family but also to the memory of loved ones who are no longer with us but whose influence continues to guide me. Their legacy inspires me to push forward and honor their impact on my life. I would like to extend my appreciation to my friends and everyone who has supported me on this journey. I am eternally grateful to my family for their unwavering belief in my potential. To my mother, thank you for your sacrifices, your love, and your faith in me, which have been my foundation and guide. You have shown me the value of hard work, resilience, and perseverance, and I am forever grateful for your guidance and support. To my friends, thank you for being a constant source of encouragement, advice, and joy. You have been my sounding boards, my advisors, and my cheerleaders. Through both challenging and rewarding moments, your humor, companionship, and insights have lightened the load and made the process more enjoyable. To everyone who has helped me along the way, whether through words of wisdom, gestures of kindness, or quiet encouragement, thank you. This accomplishment would not have been possible without your support.

ABSTRACT

Casein has many functional properties for developing food, pharmaceutical, and consumer products. However, casein precipitates around its isoelectric point of pH 4.6. Previously, increasing solutions of casein and propylene glycol alginate (PGA) to pH 11.30 followed by acidifying to pH 4.5 led to dispersions without precipitation, contributed by both covalent and non-covalent interactions. The covalent bonding is due to the transacylation reaction between ester groups of PGA and primarily amino groups of casein, and phosphate was speculated as a catalyst. The hypothesis of this thesis is that the transacylation reaction between sodium caseinate (NaCas) and PGA and therefore acid stability of dispersions is not only affected by the phosphate concentration but also cations binding electron-rich amino groups via the local ion-pairing mechanism. Solutions with 1% w/v NaCas and 1% w/v PGA were dissolved with 0, 10, 25, 50, 100 and 200 mM NaH_2PO_4, KH_2PO_4, NaCl, or KCl and were reacted at 22°C and pH 11.0 for 2 h, followed by adjusting pH to 7.0, centrifugation, and dialysis of the supernatant for analyses. A lowered degree of glycation (DOG) measured with the ortho-phthalaldehyde assay and more abundant casein bands observed in reducing gel electrophoresis at increased phosphate concentrations nullified the hypothesis of phosphate being a catalyst. The DOG was similar ($p > 0.05$) for all treatments with ≥25 mM salt, attributed to the charge screening effect. At 10 mM salt, KH_2PO_4 led to a higher DOG than KCl ($p < 0.05$), while the DOG of NaH_2PO_4 and NaCl treatments was similar ($p > 0.05$) and was lower ($p < 0.05$) than treatments with potassium. The ion-pairing mechanism was verified for the lower conductivity and thus stronger binding for NaCas solutions containing NaCl

than those with KCl. The strong binding of Na^+ with NaCas was further verified in ^{23}Na-NMR. For 10 mM treatments, precipitation was absent for all dispersions at pH 4.5 and 3.0, and the KCl treatment had the highest solubility at pH 4.5, corresponding to its fibrous structures in atomic force microscopy. The present thesis may be significant to improve functional properties of casein for food and non-food applications.

Keywords: transacylation reaction, ion effect, ion-pairing mechanism, screening effect, degree of glycation, acid solubility.

TABLE OF CONTENTS

LIST OF TABLES

LIST OF FIGURES

CHAPTER 1. MOTIVATION, HYPOTHESIS, AND OBJECTIVES

1.1. Motivation and hypothesis

Casein is a milk protein composed of four variants (Dickinson et al., 1998; Srinivasan et al., 1996) and has several techno-functional properties such as emulsification, gelation, encapsulation, and film formation (Tang et al., 2024; Yang et al., 2024; Zabot et al., 2022). Casein has been explored as a novel material for applications in food, pharmaceutical, and cosmetic products. However, casein has an isoelectric point (pI) close to pH 4.6 (Hofland et al., 1999; Moller et al., 2024) and precipitates around this acidity, limiting its application as a functional ingredient in products such as beverages (Sadiq et al., 2021). Therefore, polysaccharides are used to enhance the functionality and application of proteins in acidic products (Peng et al., 2022; Sun & Zhong, 2022). Polysaccharides can form physical complexes or covalent bonds with casein to enable the acid stability (Li & Zhong, 2022; Pan et al., 2006; Sun et al., 2018). Stabilization effectiveness depends on the intrinsic structures of the polysaccharide and the preparation method. The formed complexes may also be disintegrated or aggregate depending on environmental conditions and fundamentally colloidal interactions (Li & Zhong, 2020b). The improvement of the acidic stability of casein dispersions in acidic pH using polysaccharides to form covalent bonds is commonly studied for Maillard reaction (Barbosa et al., 2019; Hou et al., 2017; Yang et al., 2023). However, Maillard reaction produces some carcinogen byproducts and melanoidins, compounds responsible for the brown color (Hou et al., 2017). Conversely, casein micelles and polypropylene glycol alginate (PGA) going through a pH-cycle, from neutral pH to pH 11.0 and then to 4.5, formed colorless dispersions stable at pH 4.5, and the complex formation was enabled by

both covalent and non-covalent interactions (Li & Zhong, 2020b). The complex dispersions, however, became destabilized at pH lower than about 3.5, depending on the ratio of casein and PGA. At pH 11.0, casein and PGA form covalent bonds via the transacylation reaction (N. Li & Q. Zhong, 2021; Li & Zhong, 2022), and phosphate ions were speculated to function as a catalyst (Jain & Zhong, 2024; Li & Zhong, 2022). In addition, the hydration and structure of proteins in water are profoundly affected by the ionic environment to impact their reaction. More specifically, because the transacylation reaction involves electron-rich amino groups of the protein (N. Li & Q. Zhong, 2021; Li & Zhong, 2022), cations may bind with amino groups to impact the reaction. Therefore, it is hypothesized that the transacylation reaction between casein and PGA and thus the acid stability of casein can be modulated by phosphate, sodium, and potassium concentrations.

1.2. Objectives

The technological goal of this thesis is to enhance acid stability of casein by reacting with PGA. The first objective is to study the covalent modification of casein with PGA as affected by phosphate, sodium, and potassium. Casein and PGA were reacted at pH 11.0 for 2 h with different concentrations of sodium chloride (NaCl), potassium chloride (KCl), sodium phosphate monobasic (NaH_2PO_4), or potassium phosphate monobasic (KH_2PO_4). The degree of glycation and the sample structures were characterized after adjusting pH to 7.0 using hydrochloric acid. The second objective is to characterize the stability, solubility, and particle structure of dispersions after further adjusting to acidic pH.

CHAPTER 2. LITERATURE REVIEW

2.1. Structure and application of Casein

Casein represents 80% of milk protein, and bovine casein has four variants, $\alpha_{S1} - (40\%)$, $\alpha_{S2} - (10\%), \beta - (40\%), \text{and } \kappa - (10\%)$, present as colloidal particles called casein micelles (de Kruif et al., 2012; Holt et al., 2013; Pan & Zhong, 2013). The diameter of casein micelles is between 50-500 nm, with an average of 120 nm (de Kruif et al., 2012; Moller et al., 2024; Pan & Zhong, 2013). Casein micelles in bovine milk are stable after heating below 140 ºC for several minutes and compaction by ultracentrifugation and agitation but are partially disrupted by high pressure homogenization at 41-350 MPa (Schulte et al., 2020; Tang et al., 2024). However, casein micelles are unstable in acidic conditions close to the isoelectric point (pH 4.6), high pressure processing (above 200 MPa), temperatures above 140 ºC, spray drying, and slow freezing in the range from -10 to -20 ◦C due to the precipitation of calcium phosphate (Schulte et al., 2020; Tang et al., 2024). The micellar form of casein is due to the calcium phosphate linkages crosslinking phosphorylated caseins and the hydrophobic interactions (Horne, 2002; Li & Zhong, 2020b; Yang et al., 2024). Additionally, the glycomacropeptides of κ-casein contribute to the stability of micelles due to the steric and electrostatic interactions (Slattery & Evard, 1973). There are three models to describe the casein micelle structure: Sub-micelles, core-coat, and internal structure (Yang et al., 2024). The sub-micelle model is one of the classic models of casein micelles. However, this model has some limitations to describe the micelle dissociation during temperature changes and the role of κ-casein in the structure conformation and there are no evidence of sub-micelles formation (Slattery & Evard, 1973). Besides, the nanocluster structure

model provides insights into the casein conformations as a combination of spherical particles stabilized by $Ca_9(PO_4)_6$ (De Kruif & Holt, 2003). In contrast, the dual binding model offers additional information about the casein micelles elongation and aggregation via cross-linking, hydrophobic interactions and bond bridging (formation of poly-chains) (Holt, 2016). The amino acid composition of casein is responsible for the casein micelle structure. There are around 208 amino acid residues among the casein variants: 25 basic amino acids, 40 acidic amino acids, 20 aromatic amino acids, 52 non-polar amino acids, and 71 polar amino acids (Chen et al., 2024; Lauer & Baker, 1977), listed in Table 2.1. The amino groups of lysine, arginine, and histidine residues could be the reactive sites for alkaline covalent modification (Li & Zhong, 2022).

2.2. Casein-polysaccharide physical complexes to improve acid stability

The interactions between casein and different polysaccharides have been studied for applications in emulsions, encapsulation, and film formation (Li & Zhong, 2022; Sun et al., 2018). The non-covalent interactions of casein with polysaccharides involve the van der Waals forces, electrostatic, steric, hydrophobic interactions, and hydrogen bonding (Li & Zhong, 2020a). In contrast, covalent interactions involve the amide and amine bonds (N. Li & Q. Zhong, 2021). The non-covalent and covalent interactions between casein and polysaccharides can result in complexation with a decreasing level of order (Li & Zhong, 2020a).

The non-covalent interactions between proteins and polysaccharides depend on the chemical structure of the macromolecules. In general, electrostatic (attractive and repulsive), steric, and van der Waals interactions play an important role in non-covalent

interactions (Jain & Zhong, 2024; Sun et al., 2018; Zabot et al., 2022). The balance of these interactions determines if the aggregation of particles occurs in solutions. The mixture of protein and polysaccharide under or above the overlap concentration can produce one- or two-phase systems (Li & Zhong, 2020a; Soukoulis et al., 2014; Wusigale et al., 2020). The one-phase system involves the co-solubility and soluble complexes, while the two-phase system involves segregative separation and associative separation (Corredig et al., 2011). Indeed, if the concentration of the polysaccharide and protein is high, depletion and bridging flocculation due to the osmotic pressure gradient can reduce the dispersion stability (Corredig et al., 2011; Wusigale et al., 2020).

The presence of non-ionic groups such as hydroxyl or alkyl halides in the polysaccharide can affect complexation. For example, non-ionic polysaccharides such as cellulose can enhance the texture, water holding capacity and rheological properties of the protein in solution due to the formation of a strong hydrogen bonding network (Kobori et al., 2009; Ye et al., 2016). Cationic and anionic polysaccharides such as algins (carboxyl groups with pKa of 3.5), chitosan (amino groups with pKa of 6.5) and pectin (carboxyl groups with pKa of 3.5) can form complexes at different pH with the protein due to the presence of positively and negatively charged amino acids (Li & Zhong, 2020b; Maroziene & de Kruif, 2000; Mishra et al., 2024; Sun et al., 2018). pH is one of the most important factors in non-covalent interactions. Other important factors that influence the stability of complexes are the molecular weight and conformation of polysaccharides, concentrations, and ionic strength (Ding et al., 2019; Mishra et al., 2024; Wusigale et al., 2020).

2.3. Covalent casein-polysaccharide conjugates to improve acid stability

The covalent interactions between casein and polysaccharides involve crosslinking by enzymes, Maillard reaction, and nucleophilic acyl substitution reactions such as transacylation reactions (Abd El-Salam & El-Shibiny, 2020; N. Li & Q. Zhong, 2021; Li & Zhong, 2022; Sun & Zhong, 2022). The crosslinking of casein and polysaccharides by enzymes is a common method to modify proteins. Some papers have reported the modification of casein using transglutaminase and konjac glucomannan to form hybrid hydrogels for drug delivery systems (Yin et al., 2012). The modification of casein using transglutaminase also can occur with other polysaccharides such as oligochitosan and corn fiber gum, enhancing the interfacial properties (equilibrium interfacial tension), water binding capacity and solubility (Liu et al., 2018; Song & Zhao, 2014). Besides, laccase has been used to modify casein with hydrolyzed oat spelt xylan to improve techno functional properties of the protein (Selinheimo et al., 2008). However, the specificity and cost of the enzymes can limit the application of this methodology for protein modification (Yin et al., 2012).

The Maillard reaction is a sequence of non-enzymatic browning reactions (Nooshkam et al., 2019). This reaction requires the amino groups of the basic amino acids in casein and the reducing end of the polysaccharides (anomeric carbon) (Nooshkam et al., 2019). It has been reported the conjugation of casein with pectin, arabinogalactan, gum arabic, dextran, maltodextrin, and carrageenan using dry (using powders) and wet (in solutions) heating Maillard reaction method (Abd El-Salam & El-Shibiny, 2020; Seidi et al., 2023; Seo & Yoo, 2021; Shepherd et al., 2000; Yang et al., 2023). The modification using

Maillard reaction has been reported to have improved the emulsifying properties, solubility, and stability of casein (Capar & Yalcin, 2021; Shepherd et al., 2000). The cost of Maillard reaction is affordable for the food industry, but the formation of carcinogens, toxic, and sensory-alternating byproducts restricts its application in food products (Abd El-Salam & El-Shibiny, 2020).

Nucleophilic acyl substitution reactions such as transacylation reactions are the most recent novel methods to modify casein (Sun & Zhong, 2022). These reactions include the formation of amide, ester or amine bonds (Hadef, Omri, Edwards-Lévy, et al., 2017; Li & Zhong, 2022). Nucleophilic acyl substitutions reactions are a type of nucleophilic substitution in organic chemistry (Hardee et al., 2010). This reaction can occur by nucleophilic substitution, unimolecular or bimolecular depending on the nucleophilicity of the functional groups (Rossi et al., 2003). The reaction requires the presence of an electron donating group and an electro deficient center induced by the presence of carbonyl groups, ester groups, anhydrides and acid chlorides (Rossi et al., 2003). The substitution occurs in the acyl group when the leaving group is replaced by the nucleophile in the same position. In the transacylation reaction, the nucleophile is the amino group of the lysine residues of the protein that are replaced on the side chain of the ester bond of the propylene glycol alginate (PGA) (Li & Zhong, 2022). The advantages of these reactions include the reaction at room temperature, no undesirable byproducts, green solvents for reaction, and high yield (Kolb & Sharpless, 2003; Li & Zhong, 2020b). Additionally, this reaction aligns with the click chemistry principles (Kolb & Sharpless, 2003). Several studies have shown the formation of conjugates between casein and PGA

in alkaline conditions (N. Li & Q. Zhong, 2021; Sun & Zhong, 2022). However, the effect of ions (as nucleophilic attack promoters) on the degree of glycation and the stability of conjugates have not been studied.

During the transacylation reaction, not only lysine residues are available in sodium caseinate but also arginine, and histidine because they have amino groups which can have some nucleophilicity (Jain & Zhong, 2024; N. Li & Q. Zhong, 2021). However, lysine is the amino acid that is more active during the transacylation reaction due to its free amino group (N. Li & Q. Zhong, 2021).

2.4. Hofmeister effect on protein hydration

The effect of ions on the protein surface has been widely studied. Kosmotropic and chaotropic ions have an effect in the hydrogen bonding network of the protein due to the hydration shell (He & Ewing, 2023; Herman et al., 2021; Rana et al., 2023). Chaotropic ions can induce salting-in effect but kosmotropic ions can induce salting-out effect (Lai et al., 2023). In general, the Gibbs free energy of kosmotropic ions is lower than chaotropic ions due to the orderly arrangement of water molecules (Asakereh et al., 2022). Additionally, the adsorption of chaotropic ions on proteins can result in enhanced electrostatic repulsion, hydration, and salting-in effect (Lai et al., 2023; Sakai et al., 2022). The destabilization power of different ions is shown in **Fig. 2-1**.

The solvation mechanism is one of the most important factors to maintain connection between the solvent and the solute (Wei et al., 2022). However, salts can affect solvation by disturbance of the hydrogen bonding network and molecular conformation of the protein (Wei et al., 2022). The **indirect interaction mechanism** has been proposed that

the kosmotropic ions can diffuse to the second molecule water layer called the transition layer and weaken the solute-water interactions leading to salting-out. Thus, chaotropic ions are difficult to bind to water molecules in the hydration and transition layers due to their large size and low charge. Therefore, the solute-water interaction is strengthened, leading to the salting-in effect. **Direct interaction mechanism** has suggested that ions can affect different physicochemical changes of the protein such as precipitation, colloidal system, chirality, protein denaturation and stability. This is related also to the screening effect of ions at high concentrations (Wei et al., 2022).

The Triple effect mechanism involves polarization, surface tension and direct binding (Moghaddam & Thormann, 2019). The polarization includes the action of the strong hydrated kosmotropic ions in the water molecules hydrogen-bonded to the amide groups of the macromolecule (Moghaddam & Thormann, 2019). This dehydration of the amide bonds induces some polymer destabilization and salting-out (Flores et al., 2012; Moghaddam & Thormann, 2019; Rembert et al., 2012). This alteration of the polarity produces an unfavorable change in the surface tension (hydrophobic hydration) that reduces the chances of direct binding. With chaotropic ions like K^+, Na^+, and Li^+, the effect is the opposite(Chen et al., 2010; Moghaddam & Thormann, 2019).

The solute/partitioning model considers the partitioning coefficient between ions and the hydration surface of biopolymers. The model involves two thermodynamic states (Courtenay et al., 2000). The first one is swollen coil and the second collapsed globules (Moghaddam & Thormann, 2019). Further, the effect of salts on the conformational transition is analyzed by the Gibbs free energy change of the transition (Thormann,

2012). The higher the Gibbs free energy change of the transition the greater the molar surface tension. This partitioning coefficient and the free energy indicate the level of hydration of the salt and the potential excluded volume around the biopolymer surface (Felitsky & Record, 2004; Moghaddam & Thormann, 2019).

The hydration force and surface property mechanism consider the effect of electrostatic, dispersion, entropic and hydration forces (Moghaddam & Thormann, 2019), shown in **Fig 2-2**. The chaotropic ions are considered hydrophobic due to the weak interaction with water. Besides, kosmotropic ions are considered hydrophilic because of the strong interaction with water and formation of hydration shell (Dishon et al., 2009; Sivan, 2016). In this mechanism, large ions accumulate near hydrophobic surfaces, while small ions accumulate on hydrophilic surfaces (Sivan, 2016). The effect of the hydration force may depend on the distance of the ions from the charged surface and the surface properties (Sivan, 2016).

The ion specific dispersion interaction mechanism suggests that hydration entropy plays an important role in the interaction between ions and proteins, water or other molecules (Mazzini & Craig, 2019). Electrostatic and non-electrostatic contributions are important due to the electrostatic nature of the ion. For this mechanism, there is an ion-specificity which can be calculated using electrodynamic pressure forces (Moghaddam & Thormann, 2019). Besides, the hydration forces are important (Parsons & Ninham, 2011). It is considered for this mechanism that a permanent hydration layer can produce in chaotropic ions a repulsive entropic contribution (reverse ion-specific effects). Additionally, the kosmotropic ions can penetrate the hydration layer and bind to the

polymer. This mechanism does not include the solvent polarizability (Boström et al., 2002; Ninham & Yaminsky, 1997).

The electrodynamic pressure mechanism (**Fig. 2-3**) suggests that structure-stabilizing salts (kosmotropic ions) can induce a positive Lifshitz-van der Waals electrodynamic pressure (Zhao & Damodaran, 2019). In contrast, structure-destabilizing salts (chaotropic ions) can induce a negative Lifshitz-van der Waals electrodynamic pressure on proteins (Zhao & Damodaran, 2019). The pressure is related to repulsive or attractive interactions which can affect the stability of proteins in solution. These net forces are related to the size and polarizability of the ions. Therefore, the application of this mechanism is more common for anions than cations, especially at salt concentrations below 0.5 M (Zhao & Damodaran, 2019).

The ion pairing mechanism can be described for three types of ion pairs: solvent separated, solvent shared, and ion contact (Marcus & Hefter, 2006). The ion pairing mechanism involves an equilibrium between free cations, free anions, and ion pairs. The ion pairing is enthalpy-driven due to electrostatic interactions and coordinative bonding interactions which induce desolvation and formation of ion pairs (Bruce et al., 2020; van der Vegt et al., 2016). The ion pair formation also can depend on the type of ions and the competition with the solvent by partial charge neutralization (Marcus & Hefter, 2006). These interactions can be extended to interaction with ionizable groups in macromolecules such as carboxyl, amide, sulphonic, phosphate, imide, thiol, ester, aldehyde, ketone, and amine groups (Pegram & Record, 2008; van der Vegt et al., 2016).

2.5. Effect of sodium and potassium on protein surface structure

Sodium and potassium are part of the milk composition. Besides, they are the most abundant compounds in living organisms. Sodium is a smaller cation than potassium considering the ionic radius (Vrbka et al., 2006). Therefore, the specificity of sodium over potassium plays an important role not only in biochemical processes but also in the stability of biopolymers such as proteins, polysaccharides, and lipids (Baldwin, 1996). Sodium and potassium have roughly neutral Hofmeister effects but due to their different size, sodium has a slightly kosmotropic behavior and potassium a chaotropic behavior (Becconi et al., 2017). The electronic configuration of sodium is 1s2,2s2,2p6,3s1 (Three orbits) and for potassium, it is 1s2,2s2,2p6,3s2,3p6,4s1 (four orbits) (Williams, 1986). Therefore, the electronegativity and the density of charges of sodium is higher than potassium (Williams, 1986). Furthermore, sodium matches better with carboxyl, phosphate, and carbonate functional groups due to its surface charge density and local-cation specific interaction (Hess & van der Vegt, 2009). Therefore, sodium binds to functional groups in proteins stronger than potassium (salting-in and salting-out effect) (Curtis et al., 2002). It has been reported that potassium promotes the dissociation of casein in aqueous solution (Pranata et al., 2024). These facts are supported by the ion pairing mechanism which indicates that kosmotropic ions can form ion pairs better due to the charge density, electrostatic, and coordinative interactions (Bruce et al., 2020; Marcus & Hefter, 2006; van der Vegt et al., 2016). Several studies have shown the preference of sodium on the protein surface and the effect in solubility, precipitation, and stability

(Becconi et al., 2017; Vrbka et al., 2006). However, the effect of potassium ions on casein structure and stability has not been widely studied.

2.6. Ions effects on casein-polysaccharide physical complexes

The effect of ions in the formation of casein-polysaccharide physical complexes has been widely studied (Guo et al., 2023; Li & Zhong, 2020a; N. Li & Q. X. Zhong, 2021). Casein can form complexes with ionic and non-ionic polysaccharides in presence of different salts (Ding et al., 2019; Wusigale et al., 2020). Casein-chitosan complexes prepared at pH 5.5 and 0-300 mM NaCl showed an increase in flocculation at a higher ionic strength due to the electrostatic screening of monovalent ions (Ding et al., 2019). $CaCl_2$ at 0-15 mM concentrations showed an effect in the charged density of casein-carboxymethyl cellulose complexes (N. Li & Q. X. Zhong, 2021). NaCl at 100 mM showed an increase in the aggregation and reduction of stability of casein-carboxymethyl cellulose complexes due to the screening effect (N. Li & Q. X. Zhong, 2021). The presence of Na^+ and Cl^- (0.2-10 mM) showed an inhibition in the complexation of pectin and casein (Wusigale et al., 2020). The presence of Ca^{2+} (0-10 mM) showed an enhancement of the formation of the nanocomplexes between micellar casein and dextran sulfate due to the dissociation of casein micelles reducing the turbidity of the dispersions (Li & Zhong, 2020a). Casein-hydroxypropyl cellulose complexes showed better stability at pH 3.0 in presence of 2.0 mM NaCl but the increase in aggregation at, 50-100 mM NaCl (Ye et al., 2016). Therefore, the ionic environment is to be carefully studied for a specific casein-polysaccharide system.

2.7. Ion effects on forming covalent casein-polysaccharide conjugates

The effect of ions on the casein surface plays an important role during the conjugation with polysaccharides. It has been speculated that the presence of phosphate ions in the transacylation reaction increases the level of conjugation and works as a catalyst (Li & Zhong, 2022; Sun & Zhong, 2022). Cations such as sodium, lithium or potassium can induce some salting-in effect at low ionic strengths but salting-out effect at high ionic strengths (Duong-Ly & Gabelli, 2014). The presence of ions in the protein solution leads to the reduction of the Debye-length (reduction of zeta-potential) and the increase in the screening effect over the ionizable groups such as amino and carboxylate groups (Li & Zhong, 2020b). Thus, these cations can induce some screening effect in the ester groups of PGA during ester cleavage in alkaline conditions which can reduce the electrostatic repulsion and increase the chance of nucleophilic attack (Li & Zhong, 2022).

Besides, some papers have reported the beneficial effect of anions like $SO_4^{2-} > Cl^- > SCN^-$ in the mechanical and functional characteristics of soy protein/κ-carrageenan hydrogels by hydrophobic domain induced mechanism (Wang et al., 2023). The presence of $SO_4^{2-} > Cl^- > NO_3^-$ in gelatin/alginate mixtures exhibited improvement in the hydrodynamic radius and shear dependent intrinsic viscosity by Hofmeister reversal (Das et al., 2023). In contrast, $SO_4^{2-} < Cl^- < Br^- < ClO_4^- < SCN^-$ showed a decrease in viscosity and an increase in solubility of whey protein isolate in emulsions due to the reduction of flocculation degree resulting from strengthened electrostatic repulsion (Lai et al., 2023). The presence of CO_3^{2-}, citrate^{3-}, and SO_4^{2-} showed some effect in the secondary structure of pea protein, as observed for the increased emission maximum in the intrinsic

fluorescence (Liu et al., 2023). CO_3^{2-} also showed a beneficial effect in the emulsifying capacity and stability of pea protein (Liu et al., 2023). Furthermore, the effects of cations in macromolecules with amide bonds also have been analyzed (Bruce et al., 2020). $Li^+ < NH_4^+ < Mg^{2+} < K^+ < Na^+ < Ca^{2+}$ showed an increasing salting-out effect of the N-isopropylacrylamide due to the surface tension reduction resulting from Cl^- counterions and the ion pairing with chloride which reduces the interaction of cations with the amide bonds (Bruce et al., 2020). Effects of these ions on the transacylation reaction between proteins and PGA are to be studied.

2.8. Concluding remarks

Casein has some limitations in applications due to the instability in acidity close to pH 4.6 (Pan & Zhong, 2013). Therefore, covalent and non-covalent interactions with casein using other biopolymers can enhance the stability in acidic conditions and therefore functional properties (Li & Zhong, 2020a; N. Li & Q. X. Zhong, 2021). Among covalent modification methods, enzymatic reactions are costly, have low reaction rates and narrow specificity (Abd El-Salam & El-Shibiny, 2020); the Maillard reaction is difficult to control, reduces the nutritional value of the ingredients, and leads to the formation of carcinogen byproducts such as melanoidins (Barbosa et al., 2019; Yang et al., 2023); the transacylation reaction is a safe reaction that takes place at room temperature, produces transparent conjugates stable at pH 4.6, does not produce harmful byproducts, and enhances the tecno-functional properties of casein (N. Li & Q. Zhong, 2021; Sun & Zhong, 2022). However, the glycation level is limited (around 35% according to the o-phthalaldehyde assay) under current reaction conditions (Li & Zhong, 2022). Therefore,

it is important to develop strategies to enhance the glycation level by modifying reaction medium including pH and ionic strength, as well as using nucleophilic attack promoters (Li & Zhong, 2022; Sun & Zhong, 2022).

CHAPTER 3. EFFECT OF PHOSPHATE, SODIUM, AND POTASSIUM IONS ON THE TRANSACYLATION REACTION BETWEEN PROPYLENE GLYCOL ALGINATE AND SODIUM CASEINATE

3.1 Abstract

The transacylation reaction between sodium caseinate (NaCas) and propylene glycol alginate (PGA) at alkaline pH forms conjugates with improved functionalities. The objective of this study was to evaluate the influence of phosphate, sodium, and potassium ions on the degree of glycation (DOG) after reaction at pH 11.0 and 21°C for 2 h. The highest DOG was observed at 10 mM salt, following the order of KH_2PO_4 > KCl > NaH_2PO_4 = NaCl, while DOG was similar at ≥ 25 mM salt due to screening effect. The decreasing DOG at increased phosphate concentrations further nullified its role as catalyst. The stronger binding of sodium than potassium ions with NaCas as verified in ^{23}Na-NMR led to the lowered DOG. For 10 mM treatments, precipitation was absent for all dispersions at pH 4.5 and 3.0. The findings illustrate the important role of sodium and potassium ions in forming covalent NaCas-PGA conjugates.

Key words: Transacylation reaction, ion effect, degree of glycation, ion-pairing mechanism, acidic stability.

3.2. Introduction

The transacylation reaction is an advanced scalable and green reaction to produce protein-polysaccharide conjugates (N. Li & Q. Zhong, 2021; Li & Zhong, 2022; Mcdowell, 1970). The transacylation reaction involves the formation of an amide bond in alkaline conditions between the amino group of proteins and the ester group in the other macromolecule (N. Li & Q. Zhong, 2021). Conjugates formed between casein and propylene glycol alginate (PGA) have shown a high capacity of emulsifying vegetable oil, and the emulsions are stable against aggregation and phase separation under environmental stresses of pH, elevated ionic strength, and thermal processing (N. Li & Q. Zhong, 2021; Li & Zhong, 2022). Unlike the traditional Maillard reaction producing many undesirable byproducts, propylene glycol is the only generally recognized as safe byproduct in forming casein-alginate conjugates (Barbosa et al., 2019; Hadef, Omri, Edwards-Levy, et al., 2017; Li & Zhong, 2022; Sun & Zhong, 2022; Zha et al., 2021). Pea proteins after reaction with PGA have shown improvements in techno-functional properties of water solubility, water and oil binding properties, thermal stability, and emulsifying and foaming properties (Jain & Zhong, 2024). The degree of glycation (DOG) of pea protein reacting with an equal mass of PGA at pH 11.0 and 40 °C for 45 min in a sonic bath was 35.96% (Jain & Zhong, 2024), while the DOG was not quantified for casein-alginate conjugates (N. Li & Q. Zhong, 2021; Li & Zhong, 2022). The DOG in these studies should be improved to minimize unconjugated proteins.

During the transacylation reaction at alkaline pH, hydrolysis of ester bonds in PGA produces unsaturated carboxylate groups, and the attack by nucleophilic primary amine

leads to the formation of amide bonds with a partial double bond characteristic between PGA and proteins (Li & Zhong, 2022; Mckay et al., 1985). Factors affecting the nucleophilic attack therefore can impact the conjugate formation. Previously, phosphate was proposed for the potential to enhance the transacylation reaction because of its catalytic function in cleaving ester bonds (Gray et al., 1990; Kennedy et al., 1989; Li & Zhong, 2022). However, this hypothesis has not been verified.

Another factor relevant to reaction in water is the hydration properties of proteins. Besides the intrinsic protein structures, protein hydration is well known to be impacted by the type and concentration of ions in solutions. In the classical Hofmeister effect, cations and anions are classified according to the salting-in (chaotropes) and salting-out (kosmotropes) phenomena (Hofmeister, 1888; Moghaddam & Thormann, 2019; Wang et al., 2024). The power of salting-in effects follows the order of $N(CH_3)_4^+ > NH_4^+ > K^+ > Na^+ > Cs^+ > Li^+ > Mg^{2+} > Ca^{2+} > Ni^{2+}$, while the salting-out effects are in the order of $(PO_4)^{3-} > SO_4^{2-} > CH_3COO^- > Cl^- > Br^- > I^- > ClO_3^- > SCN^-$ (Mazzini & Craig, 2019; Okur et al., 2017). One of the most accepted mechanisms of monovalent cations affecting protein hydration is ion-pairing, which is described in three types: solvent separated, solvent shared, and ion contact (Marcus & Hefter, 2006). The ion-pairing mechanism involves an equilibrium between free cations, free anions and ion pairs, and it is enthalpy driven due to the electrostatic interactions and coordinative bonding interactions which induce desolvation and formation of ion pairs (Bruce et al., 2020; van der Vegt et al., 2016). The ion pair formation also depends on the type and concentration of ions and the competition with the solvent by partial charge neutralization (Jordan et al.,

2014; Marcus & Hefter, 2006). These interaction mechanisms can be extended to ionizable groups in macromolecules affecting the nucleophilic activation or deactivation of carboxyl, amide, sulphonic, phosphate, imide, thiol, ester, aldehyde, ketone, and amine groups (Pegram & Record, 2008; van der Vegt et al., 2016). However, the role of monovalent cations affecting the transacylation reaction between proteins and PGA has not been studied.

In this study, the first objective was to analyze the role of phosphate concentration on the reaction between sodium caseinate (NaCas) and PGA at pH 11.0. The second objective was to analyze the role of sodium and potassium ions during the reaction via ion-pairing mechanism. To study these effects, NaH_2PO_4 and KH_2PO_4 were studied at different concentrations and were compared to same molar concentrations of NaCl and KCl on the structures of NaCas/PGA mixtures. The third objective was to compare the solubility of reaction products as affected by ionic conditions. The present study might improve the scalability of the transacylation reaction to produce novel protein-polysaccharide conjugates for applications such as acidic beverages and natural emulsifiers. The study also can be extended to study broader scopes of anions and cations impacting the protein reaction.

3.3. Materials and methods

3.3.1. Materials

NaCas (product C8654) and sodium phosphate monobasic salt were purchased from Sigma Aldrich Corp. (St. Louis, MO). PGA (NLS-K grade, product number 2E23063) was manufactured by Kimica Corp. (Tokio, Japan). The degree of esterification of PGA

was around 88% according to the manufacturer. The potassium phosphate monobasic salt, benzoic acid, and the Pierce® bicinchoninic acid (BCA) protein assay kit were purchased from Fisher Scientific. (Pittsburgh, PA). Dialysis membrane with a molecular weight cut-off (MWCO) of 3.5 kDa (product number 132592T) was purchased from Spectrum Chemicals (Standard RC Trial Kit, Spectrum chemicals, Gardena, CA). Reagents and gels used in protein electrophoresis were purchased from Bio-Rad Laboratories, Inc. (Hercules, CA). Additional chemicals were ordered from Sigma Aldrich Corp. or Fisher Scientific.

3.3.2. Experimental methods

3.3.2.1. Transacylation reaction between NaCas and PGA

NaCas was hydrated at 1.0% w/v for 2 h in 20 mL of a solution prepared by dissolving 0, 10, 25, 50, 100 and 200 mM of NaH_2PO_4, KH_2PO_4, NaCl, or KCl in deionized water, followed by adjusting to pH 11.0 using 2.0 M NaOH or KOH for solutions with Na^+ or K^+, respectively. Subsequently, PGA powder was added gradually to the NaCas dispersion to reach an NaCas: PGA mass ratio of 1:1 or 1:2. During stirring at 990 rpm on a magnetic stirring plate for 2 h at room temperature (RT, ~21 °C), the pH of the dispersions was maintained at 11.0 by adding 2.0 M NaOH or KOH. After adjusting to pH 7.0, samples were centrifuged at 5,000 *g* for 10 min at 4 °C (Sorvall LYNX 6000 SP, Thermo Fisher Scientific, Waltham, MA) to remove any unreacted excess PGA. The supernatants adjusted to pH 7.0 with 2.0 M HCl were used in analyses or dialyzed using a membrane with MWCO of 3.5 kDa in deionized water with 0.02% w/v sodium benzoate at 4 °C to remove ions and small molecules. The dialysis process was carried out for 2

days, and the bulk water was changed every 3 h until the conductivity of the bulk water was less than 0.5 μS/cm (Orion Star A212, Thermo Fisher Scientific, Beverly, MA). A portion of the dialyzed sample was collected for subsequent analyses, and the remainder was freeze-dried using an Advantage Plus EL-85 benchtop freeze dryer (VirTis, SP Scientific, Gardiner, NY).

3.3.2.2. Absorbance at 294 and 420 nm

The supernatant samples prepared as above without dialysis were measured for absorbance at 294 and 420 nm (model UV-1900i, Shimadzu Corp., Kyoto, Japan) to analyze the presence of early-intermediate (Amadori byproducts) and advanced (melanoidins) Maillard reaction products, respectively (Dong et al., 2011; Li & Zhong, 2022). The dispersions were diluted to 0.50 mg/mL protein using deionized water before measuring the absorbance. The NaCas solution with 0.50 mg/mL protein at pH 7.0 was measured as a control.

3.3.2.3. Sodium dodecyl sulfate polyacrylamide gel electrophoresis (SDS-PAGE)

The supernatant samples prepared as above without dialysis were diluted to 0.50 mg/mL protein using deionized water. The diluted sample was mixed with an equal volume of 2X Laemmli sample buffer containing 5% β-mercaptoethanol, stirred for 30 s, and heated for 5 min at 95 ºC. Then, 10 μL of the sample after cooling to RT was loaded into wells of the Mini-PROTEAN TGX (4-20%) precast gel. The gel electrophoresis was performed at 200 V and 400 mA for 35 min, followed by staining with Coomassie blue G-250 for 2 h with gentle shaking. The gel was distained with a solution of 65% v/v water, 25% v/v

methanol, and 10% v/v acetic acid for 2 h, with the staining solution changed every 30 min until clear bands were observed.

3.3.2.4. Ortho-phthalaldehyde (OPA) assay

The DOG of the dialyzed samples prepared as above was measured using the OPA assay (Nooshkam & Madadlou, 2016). The OPA solution was prepared by dissolving 40.0 mg OPA in 1.0 mL of 95% v/v ethanol, mixed with 25 mL of 100 mM sodium tetraborate buffer (pH 9.75), 2.5 mL of 20% w/v SDS, and 100 μL of β-mercaptoethanol, and adjusted to a total volume of 50.0 mL with deionized water. The protein solutions were diluted to 1.0 mg/mL protein using deionized water. Next, 2.0 mL of the OPA solution was mixed with 100 μL of a protein sample, followed by incubation at 37 °C for 2 min. The absorbance was measured at 340 nm using the above spectrophotometer. Lysine standard was used to determine free amino group content. The DOG was calculated using eq. 1.

$$DOG\ (\%) = \left(1 - \frac{Free\ amino\ group\ content\ in\ glycated\ sample}{Free\ amino\ group\ content\ in\ nonglycated\ sample}\right) \times 100 \quad (1)$$

3.3.2.5. Size exclusion chromatography – high performance liquid chromatography (SEC-HPLC)

The SEC-HPLC was used to confirm the formation of covalent bonding between NaCas and PGA (Li & Zhong, 2022). Samples were diluted to 1.0 mg/mL protein using 50 mM sodium phosphate buffer and were filtered using 0.45 μm polytetrafluoroethylene syringe filter. After that, 25 μL of the permeate was injected to an Agilent 1200 HPLC system (Agilent Technologies, Inc., Santa Clara, CA) with a Shodex OHpak 804 HQ column (Showa Denko K.K., Tokyo, Japan). A 50 mM sodium phosphate buffer at pH 7.0

containing 5.0 mg/mL SDS was used as the mobile phase at a flow rate of 0.5 mL/min. The analysis time was 45 min, and the wavelength for absorbance measurement was 280 nm.

3.3.2.6. Zeta (ζ)-potential of the conjugates

Dispersions at pH 7.0 were diluted to 1.0 mg/mL protein with deionized water, and the diluted samples were measured for ζ-potential using a Zetasizer Nano-ZS90 instrument (Malvern Instruments Ltd., Worcestershire, UK).

3.3.2.7. Fourier-transform infrared spectroscopy (FTIR)

Lyophilized NaCas-PGA conjugates were analyzed directly using a Spectrum Two FTIR Spectrometer with a universal attenuated total reflection (ATR) accessory (PerkinElmer Inc., Waltham, MA). The spectrum analysis involved 16 scans at a resolution of 4 cm^{-1}, force gauge of 100, and wavenumber range of 2000-400 cm^{-1}. Unprocessed NaCas and PGA powders were also analyzed as controls.

3.3.2.8. Fluorescence spectroscopy

The fluorescence properties of NaCas and NaCas-PGA conjugates were evaluated using a fluorescence spectrometer (Cary Eclipse Fluorescence Spectrophotometer, Agilent, Santa Clara, CA). The lyophilized samples were dissolved in phosphate buffer (20 mM, pH 7.0) at a protein concentration of 0.10 mg/mL for the test. The excitation wavelength was set at 280 nm, and the emission wavelength range was 300-500 nm. The scanning speed was 300 nm/min, and the excitation slit width and the emission slit width were both 10 nm.

3.3.2.9. Atomic force microscopy (AFM)

AFM was used to determine the morphology of NaCas, PGA, and conjugates. Samples at pH 7.0 were diluted to 10 ppm total biopolymer concentration using deionized water, and 10 µL of the diluted sample was spread on a mica sheet. Next, samples were dried overnight before measurements using a cantilever probe with a triangular silicon tip on nitride lever with a tip radius of 650 nm at 1 Hz (model SCANASYST-AIR, Bruker Corp., Santa Barbara, CA). The scanning area was 2×2 µm, and image analysis was conducted with the NanoScope analysis software (Version 1.5, Bruker Corp., Santa Barbara, CA).

3.3.2.10. Conductivity of NaCas dispersions with NaCl and KCl

The unprocessed NaCas powder was dissolved at 1.0% w/v in deionized water pre-dissolved with 0-200 mM NaCl or KCl by stirring at 990 rpm for 2 h at RT. After adjusting to pH 7.0, the conductivity was measured using an Orion Star™ A212 Conductivity Benchtop Meter (Fisher Scientific Company, Brooklyn, NY). NaCl or KCl solutions of identical molar concentration (0-200 mM) were prepared by dissolving the respective salt in water at 990 RPM for 2 h at RT. The relative variation in conductivity (RVC) was calculated by comparing the conductivity of salt solution with (σ_1) and without (σ_2) NaCas to that following the eq. 2.

$$RVC\ (\%) = \left(\frac{\sigma_1 - \sigma_2}{\sigma_2}\right) * 100 \quad (2)$$

3.3.2.11. ^{23}Na nuclear magnetic resonance (NMR*)*

The unprocessed NaCas was hydrated at 1.0% w/v for 2 h at RT in 20 mL deionized water pre-dissolved with 0-50 mM NaCl. These samples were diluted in deuterated dimethyl sulfoxide (Sigma-Aldrich Corp., St. Louis, MO) at 5.0 mg/mL protein and

measured using a Varian VNMRS 600 MHz instrument (Bruker Corp., Billerica, MA) with a RT inverse triple resonance probe special for ^{23}Na-NMR. For the free induction decay, 256 scans were collected with a relaxation delay of 1 s and a pulse angle of 45º in the spectral width of -80 to 60 ppm.

3.3.2.12. Particle size of dispersions

The dialyzed samples were diluted to 5.0 mg/mL protein with deionized water, and the pH was adjusted to 7.0, 4.5 and 3.0 with 0.02 M HCl. The samples were photographed for visual stability. Samples were also diluted by 100 times in deionized water and adjusted to pH 7.0, 4.5, and 3.0 using 1.0 M HCl for measuring particle size using the Zetasizer Nano-ZS90 instrument (Malvern Instruments Ltd., Worcestershire, UK).

3.3.2.13. Solubility

The solubility of protein was measured using a modified method (Shen et al., 2021). The unprocessed NaCas and freeze-dried NaCas-PGA powders (10.0 mg) were mixed with 10.0 mL of deionized water and stirred at 990 rpm for 1 h at RT. Then, the pH was adjusted to 2.0-11.0 with 2.0 N HCl or NaOH. After stirring at RT for 30 min, the solutions were centrifuged with a Sorvall LYNX 6000 centrifuge (Thermo Fisher Scientific, Waltham, MA) at 4,000 *g* and 20 ºC for 20 min. The protein content of the supernatant (C_s) and the dispersions at pH 11.0 before centrifugation (C_t) was measured according to the Bradford method using bovine serum albumin as the standard (Bradford, 1976). The solubility was then calculated using eq. 2.

$$Solubility\ (\%) = \frac{C_s}{C_t} \times 100 \qquad (3)$$

3.3.2.14. Statistical Analysis

All samples were performed in triplicate independently. The statistical analysis was performed using ORIGIN® PRO for windows (Origin Lab Corporation, Northampton, MA). One way-ANOVA analysis was carried out to determine differences among means from triplicate samples, and Tukey's test was done to find out significant differences between samples at a significance level of $p < 0.05$.

3.4. Results and discussion

3.4.1. Conjugate structure assessed using SDS-PAGE and OPA assay

The effect of phosphate, sodium, and potassium ions on the reaction between NaCas and PGA analyzed with SDS-PAGE is shown in **Fig. 3.1A-G**. After the reaction, the presence of higher molecular weight mass than NaCas and the reduced intensity of the NaCas band indicates glycation via transacylation reaction, as reported previously (N. Li & Q. Zhong, 2021; Li & Zhong, 2022). At a NaCas:PGA mass ratio of 1:1, a greater amount of NaCas was conjugated at 10 and 25 mM salt than at 0, 50, 100, and 200 mM, evidenced by overall denser casein bands at higher salt concentrations (**Figure 3.1A-F**). The lower salt concentration favoring the conjugation was further evident for additional treatments at NaCas:PGA mass ratio of 1:2 and 10-25 mM salts that showed the absence of NaCas bands but smearing zones (**Fig. 3.1G**). Although more NaCas is expected to be conjugated at a higher content of PGA (mass ratio of 1:2), this observation is different from the presence of remaining NaCas bands after reaction at 50 mM NaH_2PO_4 (Li & Zhong, 2022). Therefore, low salt concentrations facilitated the conjugation.

The extent of conjugation is further compared in **Fig. 3.2A** for the DOG based on the content of free amino groups (**Fig. 3.2B**). A lower DOG was observed at a higher salt concentration, which is in general agreement with the SDS-PAGE results in **Fig. 3.1.** The DOG was not affected by the type of ions at a salt concentration of ≥25 mM ($p > 0.05$). At 10 mM salt, the KH_2PO_4 and KCl treatments showed a DOG significantly ($p < 0.05$) higher than the NaH_2PO_4 and NaCl treatments that had a similar DOG ($p > 0.05$). Overall, the DOG was the highest ($p < 0.05$) for the 10 mM KH_2PO_4 treatment. In addition, as reported previously (N. Li & Q. Zhong, 2021; Li & Zhong, 2022), the absorbance of all treatments at 294 (**Fig. 3.2C**) and 420 (**Fig. 3.2D**) nm was not higher than that of NaCas without going through the transacylation reaction, indicating the absence of Maillard reaction products. Samples prepared at 10 and 25 mM salt were therefore characterized further.

The ester groups (unsaturated carboxylate groups) of PGA present electron-deficient carbon which can be subject to nucleophilic attack (sn2) by electron-rich centers of hydroxyl and amino side groups of the protein at alkaline conditions (Li & Zhong, 2022). However, the hydrolysis of ester bonds of PGA at alkaline conditions limits the level of glycation. At higher salt concentrations, the effect of Na^+ and K^+ ions screening ionizable carbonyl groups is stronger, leading to the reduced nucleophilic attack and thus lowered DOG. The same screening effect of cations affecting nucleophilic amino groups can explain the similar DOG at the same salt concentration above 10 mM regardless of ion type (**Fig. 3.2A**). The casein band intensity in KCl and NaCl treatments and the reaction in deionized water without additional salt confirmed that the reaction can occur in

absence of phosphate ions. At 10 mM salt, the salting-in effect may be apparent, as well as the stronger effect of K^+ than Na^+ (Mazzini & Craig, 2019; Okur et al., 2017). The insignificant difference in DOG of 10 mM NaH_2PO_4 and NaCl treatments and the lower DOG at higher phosphate concentrations suggest phosphate is not a catalyst for glycation. Lastly, the highest DOG of the treatment appears to suggest the synergistic or additive effect of potassium and phosphate ions.

3.4.2. Conjugate structure assessed with SEC-HPLC and fluorescence spectra

The SEC-HPLC chromatograms of NaCas and NaCas-PGA mixtures prepared with 10-25 mM salt are presented in **Fig. 3.3.** NaCas showed a major peak appearing at a retention time of 24.47 min. At 10 mM salt, all NaCas-PGA treatments had a shorter retention time than NaCas, verifying the formation of NaCas-PGA covalent conjugates (Li & Zhong, 2022), and the KH_2PO_4 treatment showed the shortest retention time of 20.36 min (**Fig. 3.3A**), agreeing with the highest DOG (**Fig. 3.2A**). The shortened retention time of NaCas-PGA treatments was also observed at 25 mM salt concentration (**Fig. 3.3B**), but the difference among these treatments was smaller than that at 10 mM salt, agreeing with their similar DOG (**Fig. 3.2A**).

Tryptophan fluorescence is a common technique used to disclose changes of protein conformation after covalent and non-covalent modification (Jain & Zhong, 2024; Li & Zhong, 2022). The fluorescence emission spectra of NaCas and dialyzed NaCas-PGA mixtures prepared at 10 and 25 mM salt are shown in Fig. **3.3C-D**. The fluorescence intensity noticeably decreased after reacting with PGA, and the reduction was more significant at 10 mM salt. The data is overall consistent with the DOG (**Fig. 3.2A**) and

can be attributed to the covalent modification reducing the exposure of tryptophan chromophores and increasing the fluorescence quenching (Li & Zhong, 2020b). Meanwhile, the red shift of the fluorescence emission maximum occurred when NaCas was glycated with PGA (Wang et al., 2020). Changes in the polarity of the environment surrounding tryptophan residues and conformational changes around chromophores also can induce the red shift (Kuang et al., 2023). Similar results were found by Spotti et al. (2014) working with whey protein isolate and dextran sulfate and Li and Zhong (2020b) working with casein and PGA.

3.4.3. Conjugate structure assessed with FTIR

The FTIR spectra of NaCas, PGA, and NaCas-PGA conjugates produced with 10 and 25 mM salt are compared in **Fig. 3.4A** and **4B**, respectively. No noticeable differences were observed between the spectra at these two salt concentrations. The peaks at 1640 cm^{-1} and 1527 cm^{-1} in NaCas are attributed to amide I bonds (C=O stretching vibrations in the peptide bonds) and amide II bonds (C-N stretching and N-H bending vibrations), respectively (Jandura et al., 2000). The peaks at 1741 cm^{-1} and 1609 cm^{-1} in PGA are assigned to ester carbonyl (attributed to the high esterification degree in PGA) and carbonyl stretching vibrations in the polysaccharide structure (Sun et al., 2018). Some papers have reported similar results for NaCas and PGA (Jain & Zhong, 2024; Li & Zhong, 2022). The additional peak of PGA at 1033 cm^{-1} corresponds to the C-O-C, C-O, C-C stretching and O-H deformation vibration characteristic of polysaccharides with glycosidic bonds (Kuang et al., 2023; Zheng et al., 2022). The NaCas-PGA conjugates showed a combination of the NaCas and PGA peaks. The complete disappearance of the

peak at 1741 cm^{-1} in PGA suggests the complete cleavage of ester bonds after the transacylation reaction. At 10 mM salt, a significant peak shift (amide I bond) from 1640 cm^{-1} in NaCas to 1607 cm^{-1} and 1594 cm^{-1} was observed in NaCas-PGA conjugates prepared in KCl and KH_2PO_4, respectively. The amide I bond shift can be related to glycation, more significant for the KH_2PO_4 treatment with a higher DOG (**Fig. 3.2A**), and hydrophobic interactions between NaCas and PGA (Li & Zhong, 2022; Sun et al., 2018; Tavasoli et al., 2022). The amide II bond (N-H deformation) shift from 1527 cm^{-1} in NaCas to 1536, 1543, 1633, and 1532 cm^{-1} for conjugates prepared with KCl, KH_2PO_4, NaCl, and NaH_2PO_4, respectively, can be associated with electrostatic interaction between NaCas and PGA (Li & Zhong, 2020b). The FTIR analysis confirms the transacylation reaction using different salts.

3.4.4. Conjugate structures assessed with AFM

The AFM morphology of NaCas and NaCas-PGA conjugates prepared with 10 mM salt is presented in **Fig. 3.5.** The NaCas control showed small particulate structures with height around 10-15 nm (**Fig. 3.5A**). In general, the NaCas-PGA conjugates exhibited a smooth and fibrous-like structure, which was previously attributed to hydrophobic interactions and hydrogen bonding (N. Li & Q. Zhong, 2021). As shown in **Fig. 3.5B-C**, conjugates prepared with KH_2PO_4 and KCl showed fibrous structures with height of 4-10 nm and 1-1.5 nm, respectively. These fibrous and elongated structures indicate side-by-side connections and alternation of protein confirmation due to glycation (Li & Zhong, 2020b). Also, the presence of free alginate hydrolyzed from PGA may contribute to the formation of this network structure. Conjugates prepared with NaH_2PO_4 and NaCl are

displayed in **Fig. 3.5D-E**. The NaCl treatment showed similar particulate conformations to the NaCas control with height around 1-1.5 nm. However, the NaH_2PO_4 treatment exhibited a combination of structures as observed for the KCl treatment and casein particulates, with height of 4-10 nm. These results are consistent with the SDS-PAGE showing the presence of free casein molecules in the dispersions, as well as previous studies (N. Li & Q. Zhong, 2021; Li & Zhong, 2022)

3.4.5. Affinity of sodium and potassium ions to casein and relevance to the transacylation reaction

The conductivity was measured to confirm the higher affinity of Na^+ than K^+ to NaCas due to the ion-pairing mechanism (Vrbka et al., 2006), shown in **Fig. 3.6A** for RVC of NaCas solutions with 10-200 mM KCl or NaCl. The RVC of NaCas solutions with KCl was higher than the NaCl samples (Vrbka et al., 2006), indicating a lower amount of K^+ than Na^+ binding to NaCas. Na^+ has a smaller radius than K^+ (Vrbka et al., 2006), favoring the binding to proteins and therefore the lowered solution conductivity. Furthermore, because the respective electronic configuration of Na^+ and K^+ is 1s2,2s2,2p6,3s1 (three orbits) and 1s2,2s2,2p6,3s2,3p6,4s1 (four orbits) (Williams, 1986), the electronegativity and surface charge density of Na^+ is higher than K^+ (Williams, 1986), which further favors the binding of proteins by Na^+. Additionally, Na^+ matches better with carboxyl, phosphate, and carbonate functional groups than K^+ due to its surface charge density and local-cation specific interaction (Hess & van der Vegt, 2009). Thus, Na^+ binds stronger to functional groups in proteins than K^+ by coordinative bonding interactions (Curtis et al., 2002; van der Vegt et al., 2016). The ion-pairing

mechanism all together indicates the higher affinity of Na^+ than K^+ in binding to functional groups critical to the transacylation reaction (amino groups of proteins and carboxyl groups of PGA), which lowers the chance of nucleophilic attack and therefore the DOG (**Fig. 3.2A**) (Bruce et al., 2020; Dudev & Lim, 2014; Marcus & Hefter, 2006; van der Vegt et al., 2016).

The ^{23}Na-NMR was used to further understand the binding of Na^+ with NaCas at 10-50 mM NaCl and the NaCas-PGA conjugate prepared in 10 mM NaCl. As presented in **Fig. 3.6B**, a higher concentration of NaCl led to a greater peak shift to the right which can be attributed to the increasing association of Na^+ to the protein and the interaction with electro-donating carboxyl or amino groups (Okada & Lee, 2017; Yu et al., 2022). Besides, a larger peak area indicates more bound Na^+ and more stable interactions (less mobility) at a higher Na^+ concentration (Fuentes-Monteverde et al., 2021; Okada & Lee, 2017), as summarized in **Table 3.1.** Similar results at different temperatures were reported for peptides with 18-20 amino acid residues in presence of Na^+ (Fuentes-Monteverde et al., 2021). Therefore, ^{23}Na-NMR confirms the binding of Na^+ with NaCas with the ion-pairing mechanism to impact the transacylation reaction as discussed previously.

3.4.6. ζ-potential, particle size, and visual appearance of dispersions at pH 7.0, 4.5, and 3.0

The ζ-potential at pH 7.0 is shown in **Fig. 3.7** for NaCas, PGA, and NaCas-PGA conjugates prepared with 10 and 25 mM salt. The ζ-potential of NaCas-PGA conjugate dispersions (-35.7 to -37.9 mV) was higher than that of NaCas (-8.8±1.9 mV) and PGA (-

29.5±2.1 mV). The ζ-potential of conjugate dispersions is consistent with previous results (N. Li & Q. Zhong, 2021). The more negative value of the conjugates might be due to alginate attaching to casein via both covalent and non-covalent bonding (Li & Zhong, 2020b). A ζ-potential magnitude of over 30.0 mV is considered sufficient to maintain colloidal stability at pH 7.0 based on electrostatic repulsion (Hunter, 2013).

Fig. 3.7B shows the visual appearance of NaCas and NaCas-PGA dispersions prepared with 10 or 25 mM salt, adjusted to 5.0 mg/mL protein and pH 7.0, 4.5, and 3.0. All dispersions were clear at pH 7.0, while the NaCas dispersion precipitated at pH 4.5 and 3.0. All conjugate dispersions were translucent at pH 4.5. At pH 3.0, only the conjugate dispersion prepared with 25 mM NaCl showed some turbidity, which can be caused by the aggregation of the non-glycated casein that initially forms physical complexes with alginate but is detached at pH 3.0 due to protonation of carboxylate groups (N. Li & Q. X. Zhong, 2021; Ye et al., 2016).

Fig. 3.7C-D shows the Z-average diameter (D_z) of dispersions at pH 7.0, 4.5, and 3.0. NaCas and PGA had a respective D_z of 345.1±58.9 and 1284.9±325.2 nm at pH 7.0. Conjugate dispersions prepared at 10 and 25 mM KCl showed similar ($p > 0.05$) D_z at pH 4.5 and 3.0. The conjugate dispersion prepared with 25 mM NaCl showed the highest D_z at pH 3.0, leading to a more turbid dispersion (**Fig. 3.2B**). However, as previously discussed, the DOG is similar for all conjugate dispersions prepared with 25 mM salt (**Fig. 3.2A**). Although not characterized for the 25 mM treatment, the presence of particulate structures of the dispersion prepared with 10 mM NaCl at pH 7.0 (**Fig. 3.5D**) may indicate the increased tendency to aggregate at pH 3.0 than other treatments.

The particle size distributions of NaCas and NaCas-PGA dispersions prepared at 10 mM salt are presented in **Fig. 3.8A-F**. The NaCas control showed a multimodal distribution (**Fig. 3.8A**). Dispersions of NaCas-PGA prepared with KCl (**Fig. 3.8C**) and KH_2PO_4 (**Fig. 3.8D**) also showed multimodal distributions that are within the size ranges of PGA (**Fig. 3.8B**). In contrast, those prepared with NaCl (**Fig. 3.8E**) and NaH_2PO_4 (**Fig. 3.8F**) exhibited structures bigger than PGA and a new peak bigger than 2000 nm at pH 3.0, indicating aggregation. The size distributions at pH 3.0 agree with the DOG (**Fig. 3.2A**). When the DOG is sufficiently high, the electrostatic and steric repulsions resulting from the covalent attachment of alginate (after hydrolysis of ester bonds in PGA) to the protein are strong enough to resist aggregation (Li & Zhong, 2020b). In contrast, when the content of covalently attached PGA is insufficient, the increased protonation of alginate at pH below the pKa (3.5) of carboxyl groups leads to the weakened electrostatic attraction with physically complexed NaCas, leading to disintegration of complexes and aggregation of NaCas (Li & Zhong, 2020b).

3.4.7. Protein content, mass yield, and protein yield of lyophilized powders prepared with 10 mM salt

The protein content, mass yield, and protein yield of lyophilized NaCas-PGA conjugates prepared with 10 mM salt and NaCas:PGA mass ratios of 1:1 and 1:2 are shown in **Table 3.2**. In general, the protein yield did not exhibit significant differences ($p > 0.05$) to the mass yield, suggesting that the centrifugation after the reaction had a less effect on the protein than PGA. The centrifugation effect on PGA was further evident for the lower mass yield and protein yield produced at NaCas and PGA mass ratio of 1:2 than those at

1:1 ($p < 0.05$), except for the KCl treatment ($p > 0.05$) which can be correlated to the higher salting-in effect of potassium than sodium ions and the lower salting-out effect of chloride than phosphate ions. The greater centrifugation effect on PGA also led to the protein content being higher than 50% for powders produced at the NaCas:PGA mass ratio of 1:1 and higher than 33.3% at the mass ratio of 1:2. Similar results were reported after conjugating pea proteins with PGA (Jain & Zhong, 2024).

3.4.8. Water solubility of NaCas as improved by reaction with 10 mM salt

The solubility of NaCas-PGA conjugates produced with 10 mM salt in comparison to that of NaCas at pH 2.0-11.0 is shown in Fig. **3.9A-C**. NaCas exhibited low solubility at pH 3.0-4.5, which is expected at an acidity near the casein isoelectric point of pH 4.6 (Hofland et al., 1999). The NaCas-PGA conjugates prepared with KCl, KH_2PO_4, NaCl, and NaH_2PO_4 showed an increase in the solubility at pH 4.5 and 3.0, this is because the hydroxyl and carboxylate groups of the alginate moiety increase the water-protein interactions and reduces the aggregation by steric and electrostatic repulsions (Kuang et al., 2023; Seidi et al., 2023; Yao et al., 2022). Similar results have been reported in the conjugation of pea protein with PGA using 50 mM sodium phosphate buffer (Jain & Zhong, 2024).

The salt effect during the transacylation reaction improving NaCas solubility at pH 4.5 is compared in **Fig. 3.9C**. The KCl treatment showed the highest solubility ($p < 0.05$), while it was similar for the other conjugate dispersions ($p > 0.05$). The KCl treatment has the second highest DOG (**Fig. 3.2A**). Covalent conjugates are expected to have good solubility due to steric and electrostatic repulsions provided by the attached alginate (Xu

et al., 2019; Yao et al., 2022). Results in **Fig. 3.9C** suggest that physical complexes formed between free NaCas and alginate after dialysis to remove salt are important to the solubility at pH 4.5.

3.5. Conclusions

This study highlights the improvement in the DOG of NaCas-PGA conjugates prepared using the transacylation reaction at alkaline conditions leading enhanced solubility of casein. The highest DOG was achieved using 10 mM KCl and KH_2PO_4 at a NaCas:PGA mass ratio 1:2, showing the disappearance of casein bands. The phosphate ion was not critical in the DOG, while potassium ions at 10 mM improved the DOG, particularly in the form of KH_2PO_4. The less effectiveness of sodium ions in affecting the DOG was attributed to its higher affinity to form ion pairs with functional groups important to the transacylation reaction. At the studied conditions, when the ion concentration was sufficiently higher (25 mM and higher), the charge screening effect reduced the accessible reactive group to lower the DOG, regardless of the ion type. While the dispersions with a higher DOG had a higher solubility at pH 3-5, questions remain about the detailed structure of NaCas-alginate complexes after removing ions and the corresponding acid solubility.

REFERENCES

Abd El-Salam, M. H., & El-Shibiny, S. (2020). Preparation and potential applications of casein-polysaccharide conjugates: a review. *Journal of the Science of Food and Agriculture*, *100*(5), 1852-1859. https://doi.org/10.1002/jsfa.10187

Asakereh, I., Lee, K., Francisco, O. A., & Khajehpour, M. (2022). Hofmeister Effects of Group II Cations as Seen in the Unfolding of Ribonuclease A. *Chemphyschem*, *23*(12). https://doi.org/ARTN e202100884

10.1002/cphc.202100884

Baldwin, R. L. (1996). How Hofmeister ion interactions affect protein stability. *Biophysical Journal*, *71*(4), 2056-2063. https://doi.org/10.1016/S0006-3495(96)79404-3

Barbosa, J. M., Ushikubo, F. Y., Furtado, G. D., & Cunha, R. L. (2019). Oil in water emulsions stabilized by maillard conjugates of sodium caseinate-locust bean gum. *Journal of Dispersion Science and Technology*, *40*(5), 634-645. https://doi.org/10.1080/01932691.2018.1476152

Becconi, O., Ahlstrand, E., Salis, A., & Friedman, R. (2017). Protein-ion Interactions: Simulations of Bovine Serum Albumin in Physiological Solutions of NaCl, KCl and LiCl. *Israel Journal of Chemistry*, *57*(5), 403-412. https://doi.org/10.1002/ijch.201600119

Boström, M., Williams, D. R. M., & Ninham, B. W. (2002). Ion specificity of micelles explained by ionic dispersion forces. *Langmuir*, *18*(16), 6010-6014. https://doi.org/UNSP LA0201220

10.1021/la0201220

Bradford, M. M. (1976). A rapid and sensitive method for the quantitation of microgram quantities of protein utilizing the principle of protein-dye binding. *Anal Biochem*, *72*, 248-254. https://doi.org/10.1006/abio.1976.9999

Bruce, E. E., Okur, H. I., Stegmaier, S., Drexler, C. I., Rogers, B. A., van der Vegt, N. F. A., Roke, S., & Cremer, P. S. (2020). Molecular Mechanism for the Interactions of Hofmeister Cations with Macromolecules in Aqueous Solution. *Journal of the American Chemical Society*, *142*(45), 19094-19100. https://doi.org/10.1021/jacs.0c07214

Capar, T. D., & Yalcin, H. (2021). Protein/polysaccharide conjugation via Maillard reactions in an aqueous media: Impact of protein type, reaction time and temperature. *Lwt-Food Science and Technology*, *152*. https://doi.org/ARTN 112252

10.1016/j.lwt.2021.112252

Chen, X., Flores, S. C., Lim, S. M., Zhang, Y. J., Yang, T. L., Kherb, J., & Cremer, P. S. (2010). Specific Anion Effects on Water Structure Adjacent to Protein Monolayers. *Langmuir*, *26*(21), 16447-16454. https://doi.org/10.1021/la1015862

Chen, X. Q., Fan, R., Wang, Y. B., Munir, M., Li, C., Wang, C. Y., Hou, Z. Q., Zhang, G. F., Liu, L. B., & He, J. (2024). Bovine milk β-casein: Structure, properties, isolation, and targeted application of isolated products. *Comprehensive Reviews in Food Science and Food Safety*, *23*(2). https://doi.org/ARTN e13311

10.1111/1541-4337.13311

Corredig, M., Sharafbafi, N., & Kristo, E. (2011). Polysaccharide-protein interactions in dairy matrices, control and design of structures. *Food Hydrocolloids*, *25*(8), 1833-1841. https://doi.org/10.1016/j.foodhyd.2011.05.014

Courtenay, E. S., Capp, M. W., Saecker, R. M., & Record, M. T. (2000). Thermodynamic analysis of interactions between denaturants and protein surface exposed on unfolding:: Interpretation of urea and guanidinium chloride

-values and their correlation with changes in accessible surface area (ASA) using preferential interaction coefficients and the local-bulk domain model. *Proteins-Structure Function and Genetics*, 72-85. <Go to ISI>://WOS:000089784700007

Curtis, R. A., Ulrich, J., Montaser, A., Prausnitz, J. M., & Blanch, H. W. (2002). Protein-protein interactions in concentrated electrolyte solutions - Hofmeister-series effects. *Biotechnology and Bioengineering*, *79*(4), 367-380. https://doi.org/10.1002/bit.10342

Das, S., Giri, L., & Majumdar, S. (2023). Hofmeister series: An insight into its application on gelatin and alginate-based dual-drug biomaterial design. *European Polymer Journal*, *189*. https://doi.org/ARTN 111961

10.1016/j.eurpolymj.2023.111961

De Kruif, C. G., & Holt, C. (2003). Casein Micelle Structure, Functions and Interactions. In P. F. Fox & P. L. H. McSweeney (Eds.), *Advanced Dairy Chemistry—1 Proteins: Part A / Part B* (pp. 233-276). Springer US. https://doi.org/10.1007/978-1-4419-8602-3_5

de Kruif, C. G., Huppertz, T., Urban, V. S., & Petukhov, A. V. (2012). Casein micelles and their internal structure. *Advances in Colloid and Interface Science*, *171*, 36-52. https://doi.org/10.1016/j.cis.2012.01.002

Dickinson, E., Semenova, M. G., & Antipova, A. S. (1998). Salt stability of casein emulsions. *Food Hydrocolloids*, *12*(2), 227-235. https://doi.org/Doi 10.1016/S0268-005x(98)00035-6

Ding, L., Huang, Y., Cai, X. X., & Wang, S. Y. (2019). Impact of pH, ionic strength and chitosan charge density on chitosan/casein complexation and phase behavior. *Carbohydrate Polymers*, *208*, 133-141. https://doi.org/10.1016/j.carbpol.2018.12.015

Dishon, M., Zohar, O., & Sivan, U. (2009). From Repulsion to Attraction and Back to Repulsion: The Effect of NaCl, KCl, and CsCl on the Force between Silica Surfaces in Aqueous Solution. *Langmuir*, *25*(5), 2831-2836. https://doi.org/10.1021/la803022b

Dong, S. Y., Wei, B. B., Chen, B. C., Mcclements, D. J., & Decker, E. A. (2011). Chemical and Antioxidant Properties of Casein Peptide and Its Glucose Maillard Reaction Products in Fish Oil-in-Water Emulsions. *Journal of Agricultural and Food Chemistry*, *59*(24), 13311-13317. https://doi.org/10.1021/jf203778z

Dudev, T., & Lim, C. (2014). Competition among Metal Ions for Protein Binding Sites: Determinants of Metal Ion Selectivity in Proteins. *Chemical Reviews*, *114*(1), 538-556. https://doi.org/10.1021/cr4004665

Duong-Ly, K. C., & Gabelli, S. B. (2014). Salting out of Proteins Using Ammonium Sulfate Precipitation. *Laboratory Methods in Enzymology: Protein, Pt C, 541*, 85-94. https://doi.org/10.1016/B978-0-12-420119-4.00007-0

Felitsky, D. J., & Record, M. T. (2004). Application of the local-bulk partitioning and competitive binding models to interpret preferential interactions of glycine betaine and urea with protein surface. *Biochemistry*, *43*(28), 9276-9288. https://doi.org/10.1021/bi049862t

Flores, S. C., Kherb, J., Konelick, N., Chen, X., & Cremer, P. S. (2012). The Effects of Hofmeister Cations at Negatively Charged Hydrophilic Surfaces. *Journal of Physical Chemistry C*, *116*(9), 5730-5734. https://doi.org/10.1021/jp210791j

Fuentes-Monteverde, J. C., Becker, S., & Rezaei-Ghaleh, N. (2021). Biomolecular phase separation through the lens of sodium-23 NMR. *Protein Science*, *30*(7), 1315-1325. https://doi.org/10.1002/pro.4010

Gray, C. J., Griffiths, A. J., Stevenson, D. L., & Kennedy, J. F. (1990). Studies on the Chemical-Stability of Propylene-Glycol Alginate Esters. *Carbohydrate Polymers*, *12*(4), 419-430. https://doi.org/10.1016/0144-8617(90)90091-6

Guo, J. J., Zhu, S. L., Chen, P. L., Liu, Z. Y., Lin, L., & Zhang, J. (2023). Effect of physiological pH on the molecular characteristics, rheological behavior, and molecular dynamics of κ-carrageenan/casein. *Frontiers in Nutrition*, *10*. https://doi.org/ARTN 1174888

10.3389/fnut.2023.1174888

Hadef, I., Omri, M., Edwards-Levy, F., & Bliard, C. (2017). Influence of chemically modified alginate esters on the preparation of microparticles by transacylation with protein in W/O emulsions. *Carbohydrate Polymers*, *157*, 275-281. https://doi.org/10.1016/j.carbpol.2016.09.090

Hadef, I., Omri, M., Edwards-Lévy, F., & Bliard, C. (2017). Influence of chemically modified alginate esters on the preparation of microparticles by transacylation with protein in W/O emulsions. *Carbohydrate Polymers*, *157*, 275-281. https://doi.org/10.1016/j.carbpol.2016.09.090

Hardee, D. J., Kovalchuke, L., & Lambert, T. H. (2010). Nucleophilic Acyl Substitution via Aromatic Cation Activation of Carboxylic Acids: Rapid Generation of Acid Chlorides under Mild Conditions. *Journal of the American Chemical Society*, *132*(14), 5002-+. https://doi.org/10.1021/ja101292a

He, X. L., & Ewing, A. G. (2023). Hofmeister Series: From Aqueous Solution of Biomolecules to Single Cells and Nanovesicles. *Chembiochem*. https://doi.org/ARTN e202200694

10.1002/cbic.202200694

Herman, K. M., Heindel, J. P., & Xantheas, S. S. (2021). The many-body expansion for aqueous systems revisited: III. Hofmeister ion-water interactions. *Physical Chemistry Chemical Physics*, *23*(19), 11196-11210. https://doi.org/10.1039/d1cp00409c

Hess, B., & van der Vegt, N. F. A. (2009). Cation specific binding with protein surface charges. *Proceedings of the National Academy of Sciences of the United States of America*, *106*(32), 13296-13300. https://doi.org/10.1073/pnas.0902904106

Hofland, G. W., van Es, M., van der Wielen, L. A. M., & Witkamp, G. J. (1999). Isoelectric precipitation of casein using high-pressure CO. *Industrial & Engineering Chemistry Research*, *38*(12), 4919-4927. https://doi.org/10.1021/ie990136

Hofmeister, F. (1888). Zur Lehre von der Wirkung der Salze. *experimentelle Pathologie und Pharmakologie 24*, 247-260. https://doi.org/10.1007/BF01918191

Holt, C. (2016). Casein and casein micelle structures, functions and diversity in 20 species. *International Dairy Journal*, *60*, 2-13. https://doi.org/10.1016/j.idairyj.2016.01.004

Holt, C., Carver, J. A., Ecroyd, H., & Thorn, D. C. (2013). Caseins and the casein micelle: Their biological functions, structures, and behavior in foods. *Journal of Dairy Science*, *96*(10), 6127-6146. https://doi.org/10.3168/jds.2013-6831

Horne, D. S. (2002). Casein structure, self-assembly and gelation. *Current Opinion in Colloid & Interface Science*, *7*(5-6), 456-461. https://doi.org/Pii S1359-0294(02)00082-1

Doi 10.1016/S1359-0294(02)00082-1

Hou, C. C., Wu, S. F., Xia, Y. M., Phillips, G. O., & Cui, S. W. (2017). A novel emulsifier prepared from polysaccharide through Maillard reaction with casein

peptides. *Food Hydrocolloids*, *69*, 236-241. https://doi.org/10.1016/j.foodhyd.2017.01.038

Hunter, R. J. (2013). *Zeta Potential in Colloid Science*. Academic Press. https://doi.org/https://doi.org/10.1016/C2013-0-07389-6

Jain, S., & Zhong, Q. X. (2024). Enhancing the functionality of pea proteins by conjugation with propylene glycol alginate via transacylation reaction assisted with ultrasonication. *Food Chemistry*, *449*. https://doi.org/10.1016/j.foodchem.2024.139179

Jandura, P., Kokta, B. V., & Riedl, B. (2000). Fibrous long-chain organic acid cellulose esters and their characterization by diffuse reflectance FTIR spectroscopy, solid-state CP/MAS C-NMR, and X-ray diffraction. *Journal of Applied Polymer Science*, *78*(7), 1354-1365. https://doi.org/https://doi.org/10.1002/1097-4628(20001114)78:7%3C1354::AID-APP60%3E3.0.CO;2-V

Jordan, E., Roosen-Runge, F., Leibfarth, S., Zhang, F. J., Sztucki, M., Hildebrandt, A., Kohlbacher, O., & Schreiber, F. (2014). Competing Salt Effects on Phase Behavior of Protein Solutions: Tailoring of Protein Interaction by the Binding of Multivalent Ions and Charge Screening. *Journal of Physical Chemistry B*, *118*(38), 11365-11374. https://doi.org/10.1021/jp5058622

Kennedy, J. F., Griffiths, A. J., Philp, K., Stevenson, D. L., Kambanis, O., & Gray, C. J. (1989). Characteristics and Distributions of Ester Groups in Propylene-Glycol Alginates. *Carbohydrate Polymers*, *11*(1), 1-22. https://doi.org/10.1016/0144-8617(89)90040-4

Kobori, T., Matsumoto, A., & Sugiyama, S. (2009). pH-Dependent interaction between sodium caseinate and xanthan gum. *Carbohydrate Polymers*, *75*(4), 719-723. https://doi.org/10.1016/j.carbpol.2008.10.008

Kolb, H. C., & Sharpless, K. B. (2003). The growing impact of click chemistry on drug discovery. *Drug Discovery Today*, *8*(24), 1128-1137. https://doi.org/Pii S1359-6446(03)02933-7

Doi 10.1016/S1359-6446(03)02933-7

Kuang, Y., Zhao, S., Liu, P. M., Liu, M. L., Wu, K., Liu, Y., Deng, P. P., Li, C., & Jiang, F. T. (2023). Schiff base type casein-konjac glucomannan conjugates with improved stability and emulsifying properties via mild covalent cross-linking. *Food Hydrocolloids*, *141*. https://doi.org/ARTN 108733

10.1016/j.foodhyd.2023.108733

Lai, H., Shen, Q., Zhan, F. C., Jiang, S., Sui, H. M., Chen, Y. J., Li, B., & Li, J. (2023). Effect of Hofmeister series anions on freeze-thaw stability of emulsion stabilized with whey protein isolates. *Food Hydrocolloids*, *134*. https://doi.org/ARTN 108015

10.1016/j.foodhyd.2022.108015

Lauer, B. H., & Baker, B. E. (1977). Amino acid composition of casein isolated from the milks of different species. *Can J Zool*, *55*(1), 231-236. https://doi.org/10.1139/z77-026

Li, N., & Zhong, Q. (2021). Conjugation of alpha-, beta-, and kappa-Caseins with Propylene Glycol Alginate Using a Transacylation Reaction as Novel Emulsifiers.

Biomacromolecules, *22*(10), 4395-4407. https://doi.org/10.1021/acs.biomac.1c00971

Li, N., & Zhong, Q. (2022). Impacts of preparation conditions on the structure and emulsifying properties of casein-alginate conjugates produced by transacylation reaction. *Int J Biol Macromol*, *201*, 242-253. https://doi.org/10.1016/j.ijbiomac.2021.12.169

Li, N., & Zhong, Q. X. (2020a). Casein core-polysaccharide shell nanocomplexes stable at pH 4.5 enabled by chelating and complexation properties of dextran sulfate. *Food Hydrocolloids*, *103*, Article 105723. https://doi.org/10.1016/j.foodhyd.2020.105723

Li, N., & Zhong, Q. X. (2020b). Stable casein micelle dispersions at pH 4.5 enabled by propylene glycol alginate following a pH-cycle treatment. *Carbohydrate Polymers*, *233*. https://doi.org/10.1016/j.carbpol.2020.115834

Li, N., & Zhong, Q. X. (2021). Effects of polysaccharide charge density on the structure and stability of carboxymethylcellulose-casein nanocomplexes at pH 4.5 prepared with and without a pH-cycle. *Food Hydrocolloids*, *117*. https://doi.org/10.1016/j.foodhyd.2021.106718

Liu, Y., Selig, M. J., Yadav, M. P., Yin, L. J., & Abbaspourrad, A. (2018). Transglutaminase-treated conjugation of sodium caseinate and corn fiber gum hydrolysate: Interfacial and dilatational properties. *Carbohydrate Polymers*, *187*, 26-34. https://doi.org/10.1016/j.carbpol.2018.01.034

Liu, Y. X., Liu, J. M., Li, X. Y., Wei, L. K., Liu, Y. H., Lu, F. P., Wang, W. H., Li, Q. G., & Li, Y. (2023). Hofmeister anion effects synergize with microbial transglutaminase to enhance the techno-functional properties of pea protein. *Food Research International*, *169*. https://doi.org/ARTN 112824 10.1016/j.foodres.2023.112824

Marcus, Y., & Hefter, G. (2006). Ion pairing. *Chemical Reviews*, *106*(11), 4585-4621. https://doi.org/10.1021/cr040087x

Maroziene, A., & de Kruif, C. G. (2000). Interaction of pectin and casein micelles. *Food Hydrocolloids*, *14*(4), 391-394. https://doi.org/Doi 10.1016/S0268-005x(00)00019-9

Mazzini, V., & Craig, V. S. J. (2019). What is the fundamental ion-specific series for anions and cations? Ion specificity in standard partial molar volumes of electrolytes and electrostriction in water and non-aqueous solvents (vol 8, pg 7052, 2017). *Chemical Science*, *10*(11), 3430-3433. https://doi.org/10.1039/c9sc90050k

Mcdowell, R. H. (1970). New Reactions of Propylene Glycol Alginate. *Journal of the Society of Cosmetic Chemists*, *21*(7), 441-457. https://www.webofscience.com/wos/WOSCC/full-record/A1970F974600018

Mckay, J. E., Stainsby, G., & Wilson, E. L. (1985). A Comparison of the Reactivity of Alginate and Pectate Esters with Gelatin. *Carbohydrate Polymers*, *5*(3), 223-236. https://doi.org/10.1016/0144-8617(85)90024-4

Mishra, B., Pathak, D., Verma, D., & Gupta, M. K. (2024). Nanofibrous composite from chitosan-casein polyelectrolyte complex for rapid hemostasis in rat models. *International Journal of Biological Macromolecules*, *269*. https://doi.org/ARTN 131882

10.1016/j.ijbiomac.2024.131882

Moghaddam, S. Z., & Thormann, E. (2019). The Hofmeister series: Specific ion effects in aqueous polymer solutions. *Journal of Colloid and Interface Science*, *555*, 615-635. https://doi.org/10.1016/j.jcis.2019.07.067

Moller, T. L., Nielsen, S. B., Pedersen, J. S., & Corredig, M. (2024). Structural and compositional characterization of Ca- and β-casein enriched casein micelles. *Food Hydrocolloids*, *151*. https://doi.org/ARTN 109811

10.1016/j.foodhyd.2024.109811

Ninham, B. W., & Yaminsky, V. (1997). Ion binding and ion specificity: The Hofmeister effect and Onsager and Lifshitz theories. *Langmuir*, *13*(7), 2097-2108. https://doi.org/DOI 10.1021/la960974y

Nooshkam, M., & Madadlou, A. (2016). Microwave-assisted isomerisation of lactose to lactulose and Maillard conjugation of lactulose and lactose with whey proteins and peptides. *Food Chemistry*, *200*, 1-9. https://doi.org/10.1016/j.foodchem.2015.12.094

Nooshkam, M., Varidi, M., & Bashash, M. (2019). The Maillard reaction products as food-born antioxidant and antibrowning agents in model and real food systems. *Food Chemistry*, *275*, 644-660. https://doi.org/10.1016/j.foodchem.2018.09.083

Okada, K. S., & Lee, Y. (2017). Characterization of Sodium Mobility and Binding by Na NMR Spectroscopy in a Model Lipoproteic Emulsion Gel for Sodium Reduction. *Journal of Food Science*, *82*(7), 1563-1568. https://doi.org/10.1111/1750-3841.13750

Okur, H. I., Hladílková, J., Rembert, K. B., Cho, Y., Heyda, J., Dzubiella, J., Cremer, P. S., & Jungwirth, P. (2017). Beyond the Hofmeister Series: Ion-Specific Effects on Proteins and Their Biological Functions. *Journal of Physical Chemistry B*, *121*(9), 1997-2014. https://doi.org/10.1021/acs.jpcb.6b10797

Pan, K., & Zhong, Q. X. (2013). Improving Clarity and Stability of Skim Milk Powder Dispersions by Dissociation of Casein Micelles at pH 11.0 and Acidification with Citric Acid. *Journal of Agricultural and Food Chemistry*, *61*(38), 9260-9268. https://doi.org/10.1021/jf402870y

Pan, X. Y., Mu, M. F., Hu, B., Yao, P., & Jiang, M. (2006). Micellization of casein-graft-dextran copolymer prepared through Maillard reaction. *Biopolymers*, *81*(1), 29-38. https://doi.org/10.1002/bip.20372

Parsons, D. F., & Ninham, B. W. (2011). Surface charge reversal and hydration forces explained by ionic dispersion forces and surface hydration. *Colloids and Surfaces a-Physicochemical and Engineering Aspects*, *383*(1-3), 2-9. https://doi.org/10.1016/j.colsurfa.2010.12.025

Pegram, L. M., & Record, M. T. (2008). Thermodynamic origin of Hofmeister ion effects. *Journal of Physical Chemistry B*, *112*(31), 9428-9436. https://doi.org/10.1021/jp800816a

Peng, B. S., Li, Z. H., Xiong, Q. M., Wu, C. D., Huang, J., Zhou, R. Q., & Jin, Y. (2022). Casein-dextran complexes subjected to microfiltration: Colloidal properties and their corresponding processing behaviors. *Journal of Food Engineering*, *320*, Article 110913. https://doi.org/10.1016/j.jfoodeng.2021.110913

Pranata, J., Hoyt, H., Drake, M., & Barbano, D. M. (2024). Effect of dipotassium phosphate addition and heat on proteins and minerals in milk protein beverages. *Journal of Dairy Science*, *107*(2), 695-710. https://doi.org/10.3168/jds.2023-23768

Rana, B., Fairhurst, D. J., & Jena, K. C. (2023). Ion-Specific Water-Macromolecule Interactions at the Air/Aqueous Interface: An Insight into Hofmeister Effect. *Journal of the American Chemical Society*, *145*(17), 9646-9654. https://doi.org/10.1021/jacs.3c00701

Rembert, K. B., Paterová, J., Heyda, J., Hilty, C., Jungwirth, P., & Cremer, P. S. (2012). Molecular Mechanisms of Ion-Specific Effects on Proteins. *Journal of the American Chemical Society*, *134*(24), 10039-10046. https://doi.org/10.1021/ja301297g

Rossi, R. A., Pierini, A. B., & Peñéñory, A. B. (2003). Nucleophilic substitution reactions by electron transfer. *Chemical Reviews*, *103*(1), 71-167. https://doi.org/10.1021/cr960134o

Sadiq, U., Gill, H., & Chandrapala, J. (2021). Casein micelles as an emerging delivery system for bioactive food components. *Foods*, *10*(8), 1965.

Sakai, K., Sato, Y., Okada, M., & Yamaguchi, S. (2022). Enhanced activity and stability of protein-glutaminase by Hofmeister effects. *Molecular Catalysis*, *517*. https://doi.org/ARTN 112054

10.1016/j.mcat.2021.112054

Schulte, J., Stöckermann, M., & Gebhardt, R. (2020). Influence of pH on the stability and structure of single casein microparticles. *Food Hydrocolloids*, *105*. https://doi.org/ARTN 105741

10.1016/j.foodhyd.2020.105741

Seidi, P., Nasirpour, A., Keramat, J., & Saeidy, S. (2023). Functional and structural properties of gum arabic complexes with casein and hydrolyzed casein achieved by Maillard reaction. *Journal of Dispersion Science and Technology*, *44*(4), 639-650. https://doi.org/10.1080/01932691.2021.1958686

Selinheimo, E., Lampila, P., Mattinen, M. L., & Buchert, J. (2008). Formation of protein - Oligosaccharide conjugates by laccase and tyrosinase. *Journal of Agricultural and Food Chemistry*, *56*(9), 3118-3128. https://doi.org/10.1021/jf0730791

Seo, C. W., & Yoo, B. (2021). Preparation of milk protein isolate/κ-carrageenan conjugates by maillard reaction in wet-heating system and their application to stabilization of oil-in-water emulsions. *Lwt-Food Science and Technology*, *139*. https://doi.org/ARTN 110542

10.1016/j.lwt.2020.110542

Shen, Y. T., Tang, X., & Li, Y. H. (2021). Drying methods affect physicochemical and functional properties of quinoa protein isolate. *Food Chemistry*, *339*. https://doi.org/10.1016/j.foodchem.2020.127823

Shepherd, R., Robertson, A., & Ofman, D. (2000). Dairy glycoconjugate emulsifiers: casein-maltodextrins. *Food Hydrocolloids*, *14*(4), 281-286. https://doi.org/Doi 10.1016/S0268-005x(99)00067-3

Sivan, U. (2016). The inevitable accumulation of large ions and neutral molecules near hydrophobic surfaces and small ions near hydrophilic ones. *Current Opinion in Colloid & Interface Science*, *22*, 1-7. https://doi.org/10.1016/j.cocis.2016.02.004

Slattery, C. W., & Evard, R. (1973). A model for the formation and structure of casein micelles from subunits of variable composition. *Biochim Biophys Acta*, *317*(2), 529-538. https://doi.org/10.1016/0005-2795(73)90246-8

Song, C. L., & Zhao, X. H. (2014). The preparation of an oligochitosan-glycosylated and cross-linked caseinate obtained by a microbial transglutaminase and its functional properties. *International Journal of Dairy Technology*, *67*(1), 110-116. https://doi.org/10.1111/1471-0307.12091

Soukoulis, C., Behboudi-Jobbehdar, S., Yonekura, L., Parmenter, C., & Fisk, I. (2014). Impact of Milk Protein Type on the Viability and Storage Stability of Microencapsulated

NCIMB 701748 Using Spray Drying. *Food and Bioprocess Technology*, *7*(5), 1255-1268. https://doi.org/10.1007/s11947-013-1120-x

Spotti, M. J., Martinez, M. J., Pilosof, A. M. R., Candioti, M., Rubiolo, A. C., & Carrara, C. R. (2014). Influence of Maillard conjugation on structural characteristics and rheological properties of whey protein/dextran systems. *Food Hydrocolloids*, *39*, 223-230. https://doi.org/10.1016/j.foodhyd.2014.01.014

Srinivasan, M., Singh, H., & Munro, P. A. (1996). Sodium caseinate-stabilized emulsions: Factors affecting coverage and composition of surface proteins. *Journal of Agricultural and Food Chemistry*, *44*(12), 3807-3811. https://doi.org/DOI 10.1021/jf960135h

Sun, C. X., Gao, Y. X., & Zhong, Q. X. (2018). Properties of Ternary Biopolymer Nanocomplexes of Zein, Sodium Caseinate, and Propylene Glycol Alginate and Their Functions of Stabilizing High Internal Phase Pickering Emulsions. *Langmuir*, *34*(31), 9215-9227. https://doi.org/10.1021/acs.langmuir.8b01887

Sun, C. X., & Zhong, Q. X. (2022). Alkaline conjugation of caseinate and propylene glycol alginate to prepare biopolymer complexes stabilizing oil-in-water emulsion gels. *Food Hydrocolloids*, *123*. https://doi.org/10.1016/j.foodhyd.2021.107192

Tang, Q., Roos, Y. H., Vahedikia, N., & Miao, S. (2024). Evaluation on pH-dependent thermal gelation performance of chickpea, pea protein, and casein micelles. *Food Hydrocolloids*, *149*. https://doi.org/ARTN 109618

10.1016/j.foodhyd.2023.109618

Tavasoli, S., Maghsoudlou, Y., Jafari, S. M., & Tabarestani, H. S. (2022). Improving the emulsifying properties of sodium caseinate through conjugation with soybean

soluble polysaccharides. *Food Chemistry*, *377*. https://doi.org/10.1016/j.foodchem.2021.131987

Thormann, E. (2012). On understanding of the Hofmeister effect: how addition of salt alters the stability of temperature responsive polymers in aqueous solutions. *RSC Advances*(22), 8297-8305. https://doi.org/10.1039/C2RA20164J

van der Vegt, N. F. A., Haldrup, K., Roke, S., Zheng, J. R., Lund, M., & Bakker, H. J. (2016). Water-Mediated Ion Pairing: Occurrence and Relevance. *Chemical Reviews*, *116*(13), 7626-7641. https://doi.org/10.1021/acs.chemrev.5b00742

Vrbka, L., Vondrásek, J., Jagoda-Cwiklik, B., Vácha, R., & Jungwirth, P. (2006). Quantification and rationalization of the higher affinity of sodium over potassium to protein surfaces. *Proceedings of the National Academy of Sciences of the United States of America*, *103*(42), 15440-15444. https://doi.org/10.1073/pnas.0606959103

Wang, L. X., Zhang, S. L., Jiang, W. P., Zhao, H. Y., & Fu, J. J. (2020). Ability of casein hydrolysate-carboxymethyl chitosan conjugates to stabilize a nanoemulsion: Improved freeze-thaw and pH stability. *Food Hydrocolloids*, *101*. https://doi.org/10.1016/j.foodhyd.2019.105452

Wang, L. Y., Dong, Y. B., Wang, L., Cui, M. Q., Zhang, Y., Jiang, L. Z., & Sui, X. A. (2023). Elucidating the effect of the Hofmeister effect on formation and rheological properties of soy protein/κ-carrageenan hydrogels. *Food Hydrocolloids*, *143*. https://doi.org/ARTN 108905

10.1016/j.foodhyd.2023.108905

Wang, Z. M., Lan, T. T., Jiang, J., Song, T. Y., Liu, J. S., Zhang, H., & Lin, K. (2024). On the modification of plant proteins: Traditional methods and the Hofmeister effect. *Food Chemistry*, *451*. https://doi.org/10.1016/j.foodchem.2024.139530

Wei, W. C., Chen, X. J., & Wang, X. J. (2022). Nanopore Sensing Technique for Studying the Hofmeister Effect. *Small*, *18*(23). https://doi.org/ARTN 2200921 10.1002/smll.202200921

Williams, R. J. P. (1986). The Biochemistry of Sodium, Potassium, Magnesium, and Calcium. *Current Contents/Engineering Technology & Applied Sciences*(1), 16-16. https://www.webofscience.com/wos/WOSCC/full-record/A1986AWK9600001

Wusigale, Liang, L., & Luo, Y. C. (2020). Casein and pectin: Structures, interactions, and applications. *Trends in Food Science & Technology*, *97*, 391-403. https://doi.org/10.1016/j.tifs.2020.01.027

Xu, H. X., Zhang, T. T., Lu, Y. Q., Lin, X., Hu, X. P., Liu, L. Z., He, Z. D., & Wu, X. L. (2019). Effect of chlorogenic acid covalent conjugation on the allergenicity, digestibility and functional properties of whey protein. *Food Chemistry*, *298*. https://doi.org/10.1016/j.foodchem.2019.125024

Yang, S., Zhang, G., Chu, H., Du, P., Li, A., Liu, L., & Li, C. (2023). Changes in the functional properties of casein conjugates prepared by Maillard reaction with pectin or arabinogalactan. *Food Research International*, *165*, 112510. https://doi.org/10.1016/j.foodres.2023.112510

Yang, Y. X., Xu, Q. N., Wang, X. Y., Bai, Z. X., Xu, X. Y., & Ma, J. Z. (2024). Casein-based hydrogels: Advances and prospects. *Food Chemistry*, *447*. https://doi.org/ARTN 138956

10.1016/j.foodchem.2024.138956

Yao, X., McClements, D. J., Su, Y. J., Li, J. H., Chang, C. H., Wang, J., Yang, Y. J., & Gu, L. P. (2022). Fabrication, Structural and Emulsifying Properties of Egg White Protein-Dextran Conjugates through Maillard Reaction. *Food Biophysics*, *17*(4), 650-661. https://doi.org/10.1007/s11483-022-09745-8

Ye, R., Cheng, Q. K., Cai, J. C., Feng, T., & Wang, G. Y. (2016). Stable Casein-Hydroxypropyl Cellulose Complexes at Low pH. *Journal of Food Quality*, *39*(4), 292-300. https://doi.org/10.1111/jfq.12197

Yin, W. W., Su, R. X., Qi, W., & He, Z. M. (2012). A casein-polysaccharide hybrid hydrogel cross-linked by transglutaminase for drug delivery. *Journal of Materials Science*, *47*(4), 2045-2055. https://doi.org/10.1007/s10853-011-6005-7

Yu, B. H., Bien, K. G., Pletka, C. C., & Iwahara, J. (2022). Dynamics of Cations around DNA and Protein as Revealed by Na Diffusion NMR Spectroscopy. *Analytical Chemistry*, *94*(5), 2444-2452. https://doi.org/10.1021/acs.analchem.1c04197

Zabot, G. L., Rodrigues, F. S., Ody, L. P., Tres, M. V., Herrera, E., Palacin, H., Córdova-Ramos, J. S., Best, I., & Olivera-Montenegro, L. (2022). Encapsulation of Bioactive Compounds for Food and Agricultural Applications. *Polymers*, *14*(19). https://doi.org/ARTN 4194

10.3390/polym14194194

Zha, F. C., Dong, S. Y., Rao, J. J., & Chen, B. C. (2021). Pea protein isolate-gum Arabic Maillard conjugates improves physical and oxidative stability of oil-in-water emulsions (vol 285, pg 130, 2019). *Food Chemistry, 364*. https://doi.org/10.1016/j.foodchem.2021.130717

Zhao, L., & Damodaran, S. (2019). Hofmeister Order of Anions on Protein Stability Originates from Lifshitz-van der Waals Dispersion Interaction with the Protein Phase. *Langmuir, 35*(40), 12993-13002. https://doi.org/10.1021/acs.langmuir.9b00486

Zheng, Y. M., Chang, Y., Luo, B. Y., Teng, H., & Chen, L. (2022). Molecular structure modification of ovalbumin through controlled glycosylation with dextran for its emulsibility improvement. *International Journal of Biological Macromolecules*, *194*, 1-8. https://doi.org/10.1016/j.ijbiomac.2021.11.130

Appendix

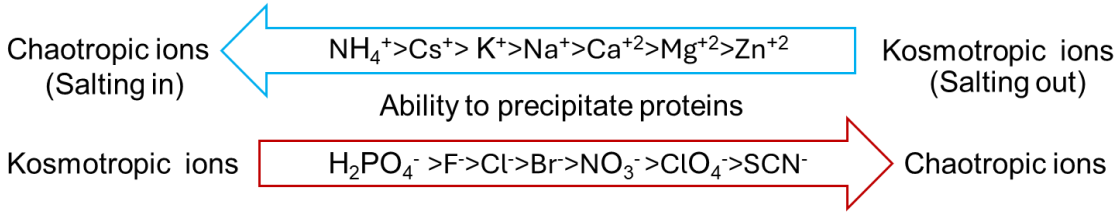

Figure 2.1. The Hofmeister series organized by destabilization power. Figure is redrawn from a reference (He & Ewing, 2023).

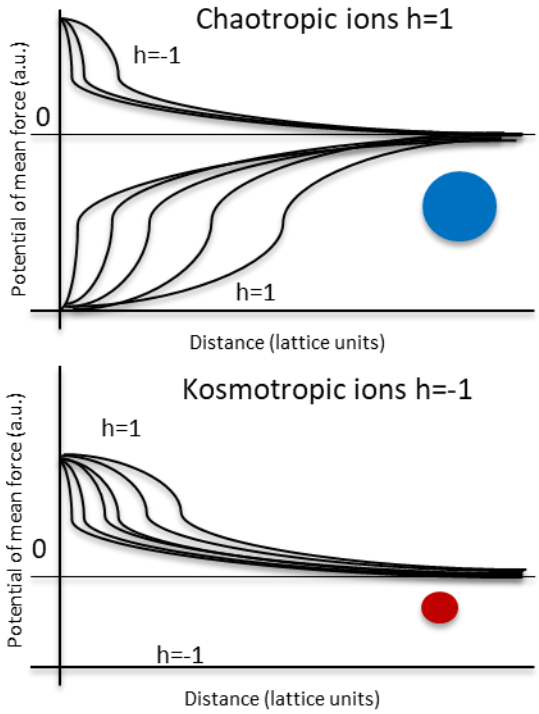

Figure 2.2. Description of Hofmeister series for surfaces with different polarities and charges. Positive potential means hydrophilic and negative potential means hydrophobic. Figures are redrawn from a reference (Sivan, 2016).

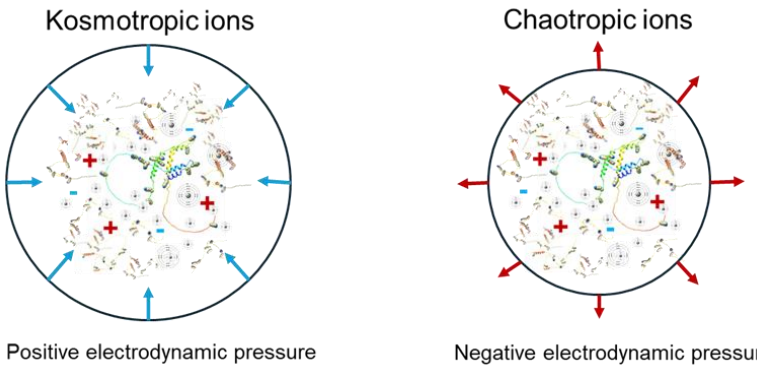

Figure 2.3. Lifshitz-van der Waals electrodynamic pressure of kosmotropic and chaotropic ions and the impact on casein micelle structure. Illustrations are redrawn based on concepts in a reference (Zhao & Damodaran, 2019).

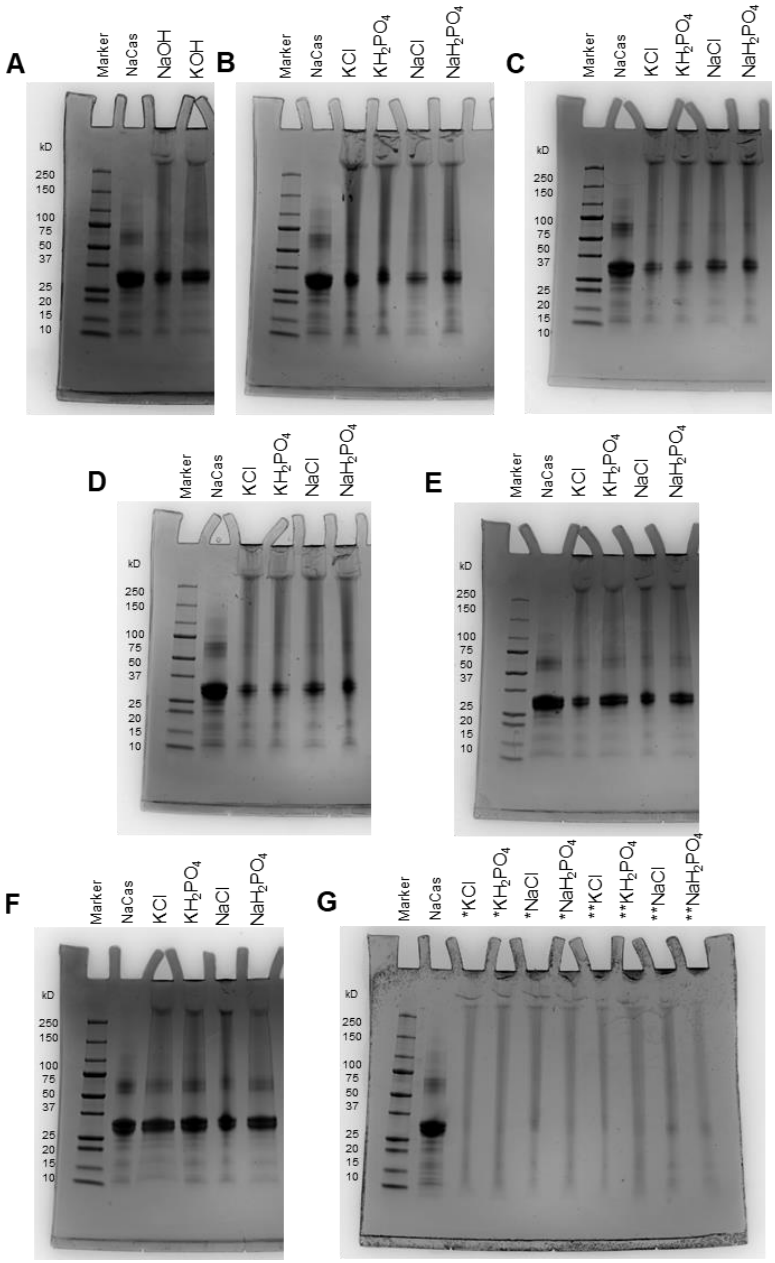

Figure 3.1. SDS-PAGE analysis of sodium caseinate (NaCas) and its mixture with propylene glycol alginate (PGA) at mass ratio of 1:1 after incubation at pH 11.0 and 0 (A), 10 (B), 25 (C), 50 (D), 100 (E), or 200 (F) mM of different salts for 2 h, followed by pH shifting to 7.0, centrifugation at 5000 *g* for 10 min, and taking the supernatant for analysis . Each well was loaded with 10 µg of protein. Figure G shows comparable treatments with NaCas:PGA mass ratio of 1:2 after reaction with 10 (*) or 25 (**) mM of different salts.

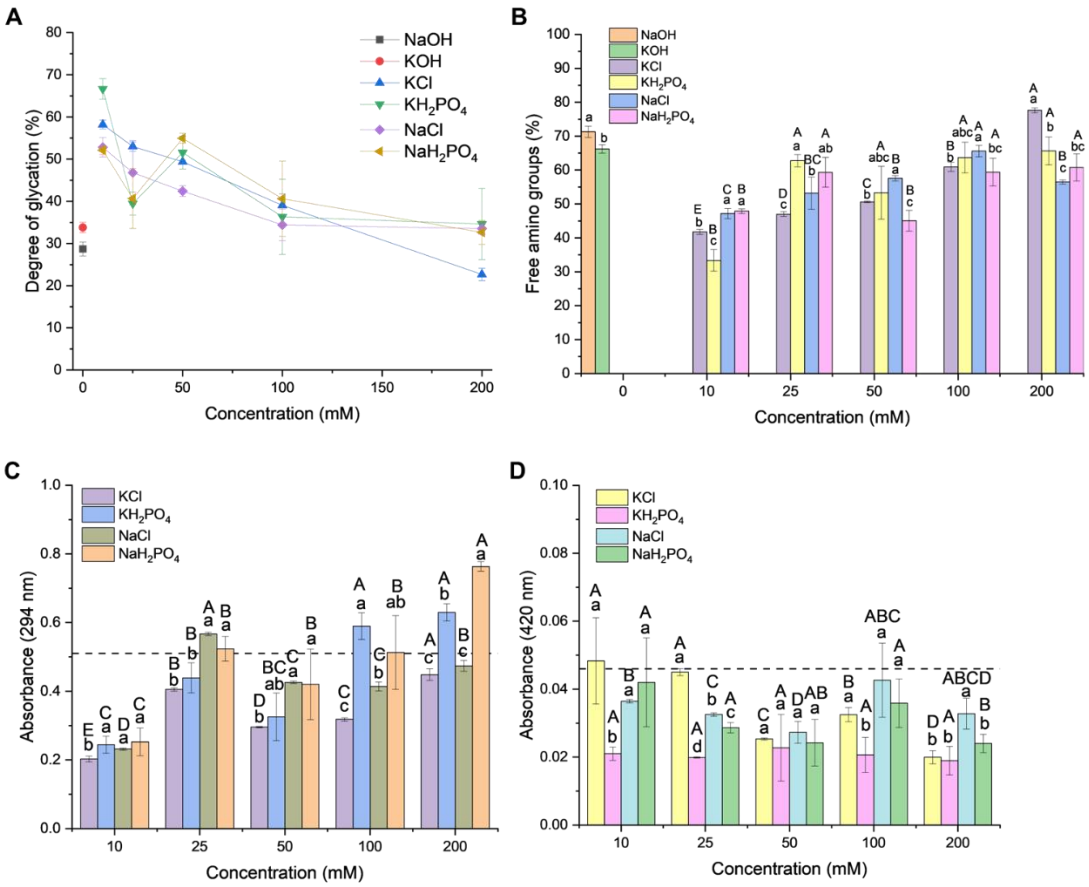
A
Degree of glycation (%)
Concentration (mM)
NaOH
KOH
KCl
KH2PO4
NaCl
NaH2PO4
B
Free amino groups (%)
Concentration (mM)
C
Absorbance (294 nm)
Concentration (mM)
D
Absorbance (420 nm)
Concentration (mM)

Figure 3.2. The degree of glycation (A), free amino group% in reference to the unprocessed sodium caseinate (NaCas; B), the absorbance at 294 nm (C) and 420 nm (D) of NaCas-propylene glycol alginate (1:1, w:w) after incubation for 2 h at pH 11.0 and 10-200 mM KCl, KH_2PO_4, NaCl, or NaH_2PO_4, followed by pH shifting to 7.0 and centrifugation at 5000 *g* for 10 min to take the supernatant for dialysis and analysis. The NaOH and KOH treatments in (A) and (B) are prepared without additional salt and with the pH adjusted to 11.0 with NaOH and KOH solution, respectively. Samples in (C) and (D) are adjusted to 5.0 mg/mL protein for analysis, with the dashed line being the same concentration of unprocessed NaCas at pH 7.0. SDs in (B) are shown in error bars (n = 3). Different lowercase and uppercase letters above the bars in (B-D) stand for significant differences ($p < 0.05$) between treatments with the same concentration of different salts and the same salt at different concentrations, respectively.

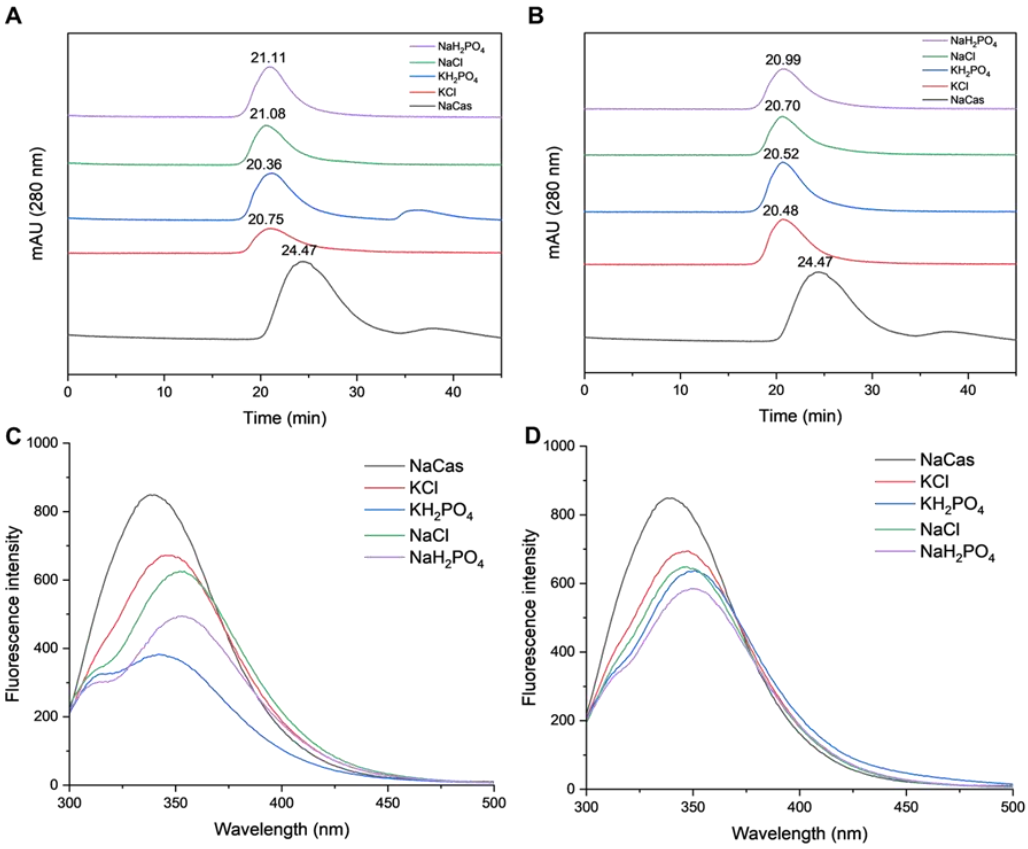

Figure 3.3. SEC-HPLC chromatograms (A and B) and fluorescence spectra (C and D) of sodium caseinate (NaCas) and NaCas-propylene glycol alginate mixture (1:1, w:w) after reaction for 2 h at pH 11.0 and 10 (A, C) or 25 (B, D) mM of different salts, followed by pH shifting to 7.0 and centrifugation at 5000 *g* for 10 min to take the supernatant for dialysis and analysis at 2.0 mg/mL protein.

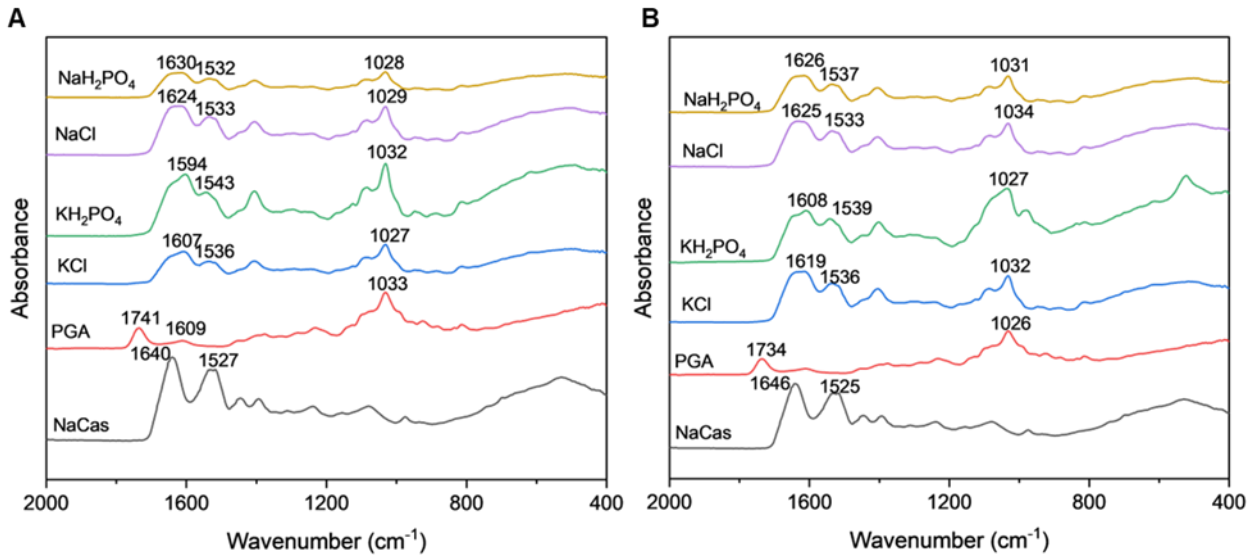

Figure 3.4. FTIR spectra of unprocessed sodium caseinate (NaCas), propylene glycol alginate (PGA), and their mixture (1:1, w:w) after reaction for 2 h at pH 11.0 and 10 (A) or 25 (B) mM of different salts, centrifugation at 5000 *g* for 10 min, and lyophilization of the dialyzed supernatant.

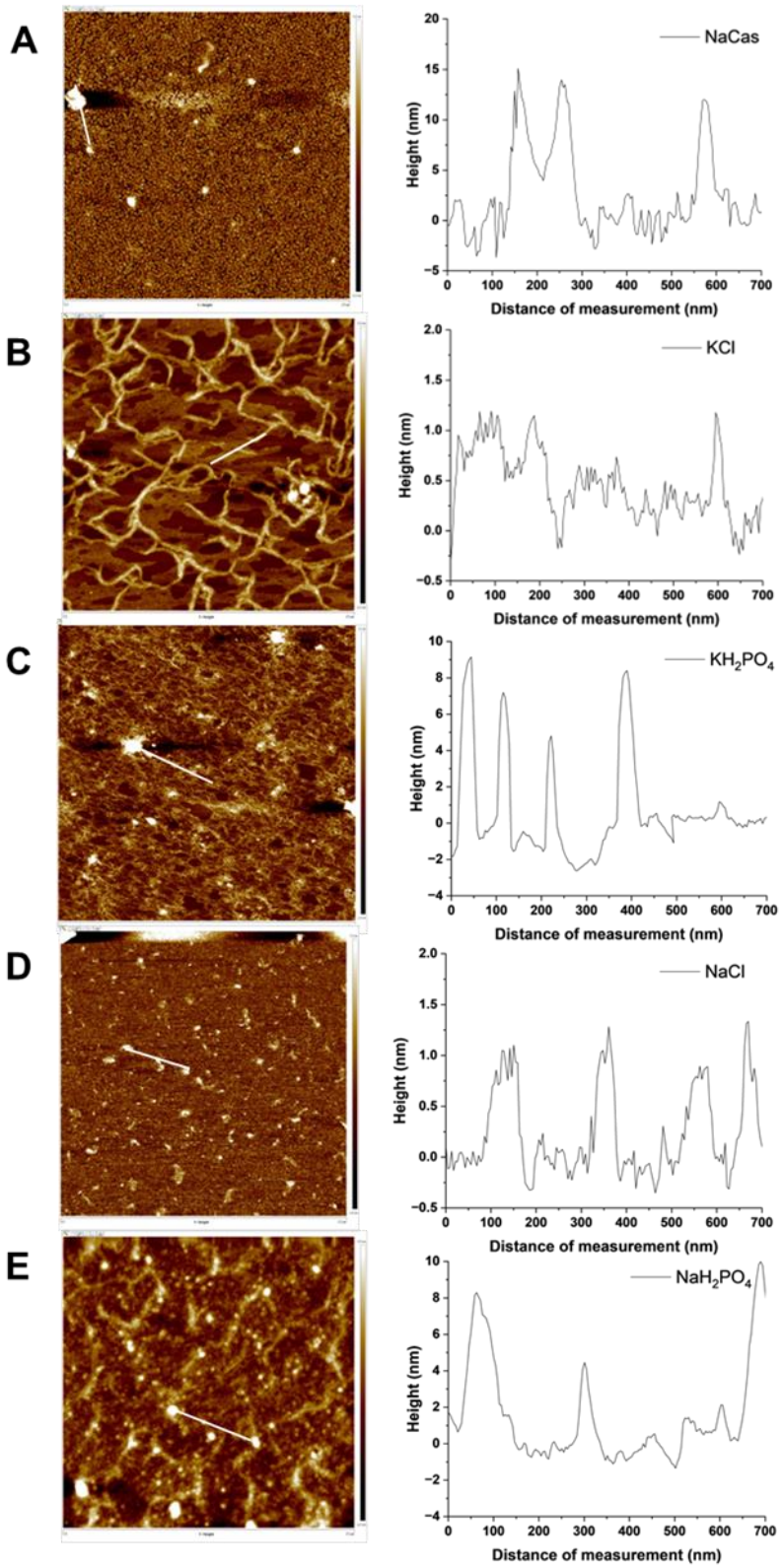
A
B
C
D
E
NaCas
KCl
KH_2PO_4
NaCl
NaH_2PO_4
Height (nm)
Distance of measurement (nm)

Figure 3.5. AFM images (2000 × 2000 nm) in height modulus channel and height distribution of structures along the white lines of NaCas (A) and its mixture with an equal mass of propylene glycol alginate after reaction for 2 h at pH 11.0 and 10 mM KCl (B), KH_2PO_4 (C), NaCl (D), or NaH_2PO_4 (E), followed by pH shifting to 7.0 and centrifugation at 5000 *g* for 10 min to take the supernatant for dialysis and analysis at 0.001% w/v biopolymer.

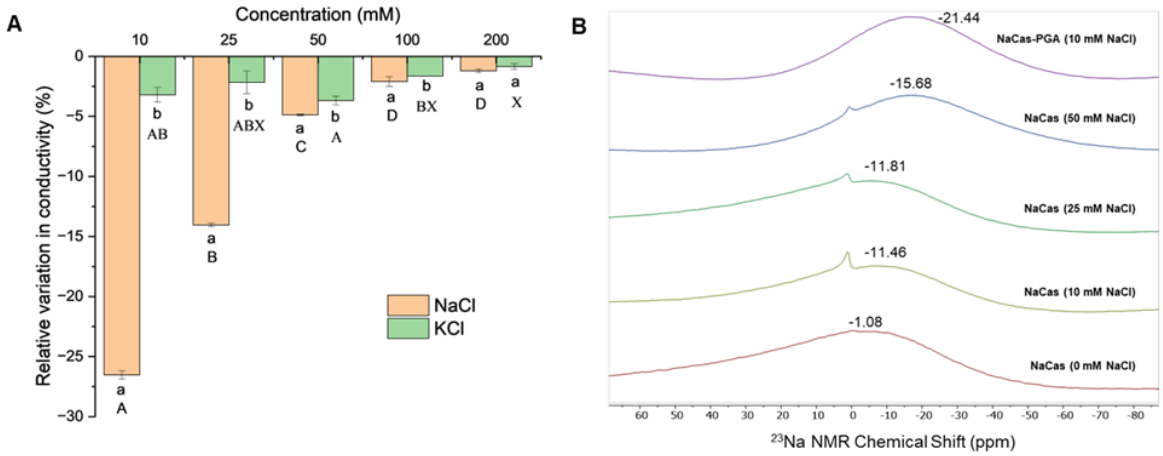

Figure 3.6. Relative variation in conductivity (A) and ^{23}Na-NMR spectra (B) of sodium caseinate (NaCas) hydrated at 1.6% w/v in deionized water with 10-200 mM KCl or NaCl for 2 h. The NaCas-propylene glycol alginate (PGA) sample (1:1, w:w) in B is produced after reaction for 2 h at pH 11.0 and 10 mM NaCl. SDs in (A) are shown in error bars (n = 3). Same lowercase and uppercase letters above the bars in (A) stand for significance differences ($p < 0.05$) between treatments with the same concentration of different salts and the same salt at different concentrations, respectively.

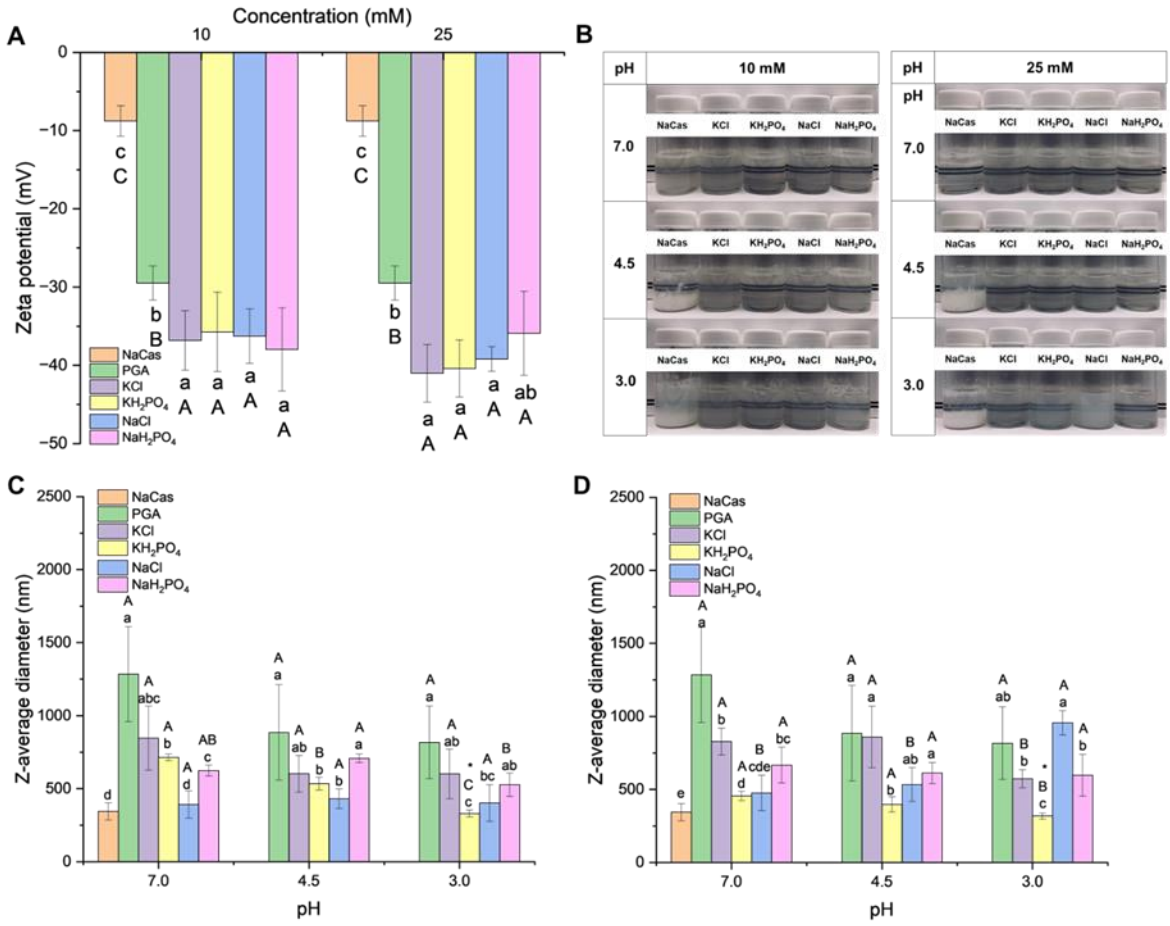

Figure 3.7. Zeta-potential at pH 7.0 (A), visual appearance at 5.0 mg/mL protein (B), and Z-average diameter (C – 10 mM; D – 25 mM) at pH 7.0, 4.5, 3.0 for sodium caseinate (NaCas; not measured at pH 4.5 and 3.0 due to precipitation), propylene glycol alginate (PGA), and NaCas-PGA mixture (1:1, w:w) after reaction for 2 h at pH 11.0 and 10 or 25 mM of different salts, followed by pH shifting to 7.0 and centrifugation at 5000 *g* for 10 min to take the supernatant for dialysis and analysis. SDs are shown in error bars (n = 3). Same lowercase and uppercase letters above the bars in A, C, and D stand for significant differences ($p < 0.05$) between treatments with the same concentration of different salts and the same salt at different concentrations, respectively.

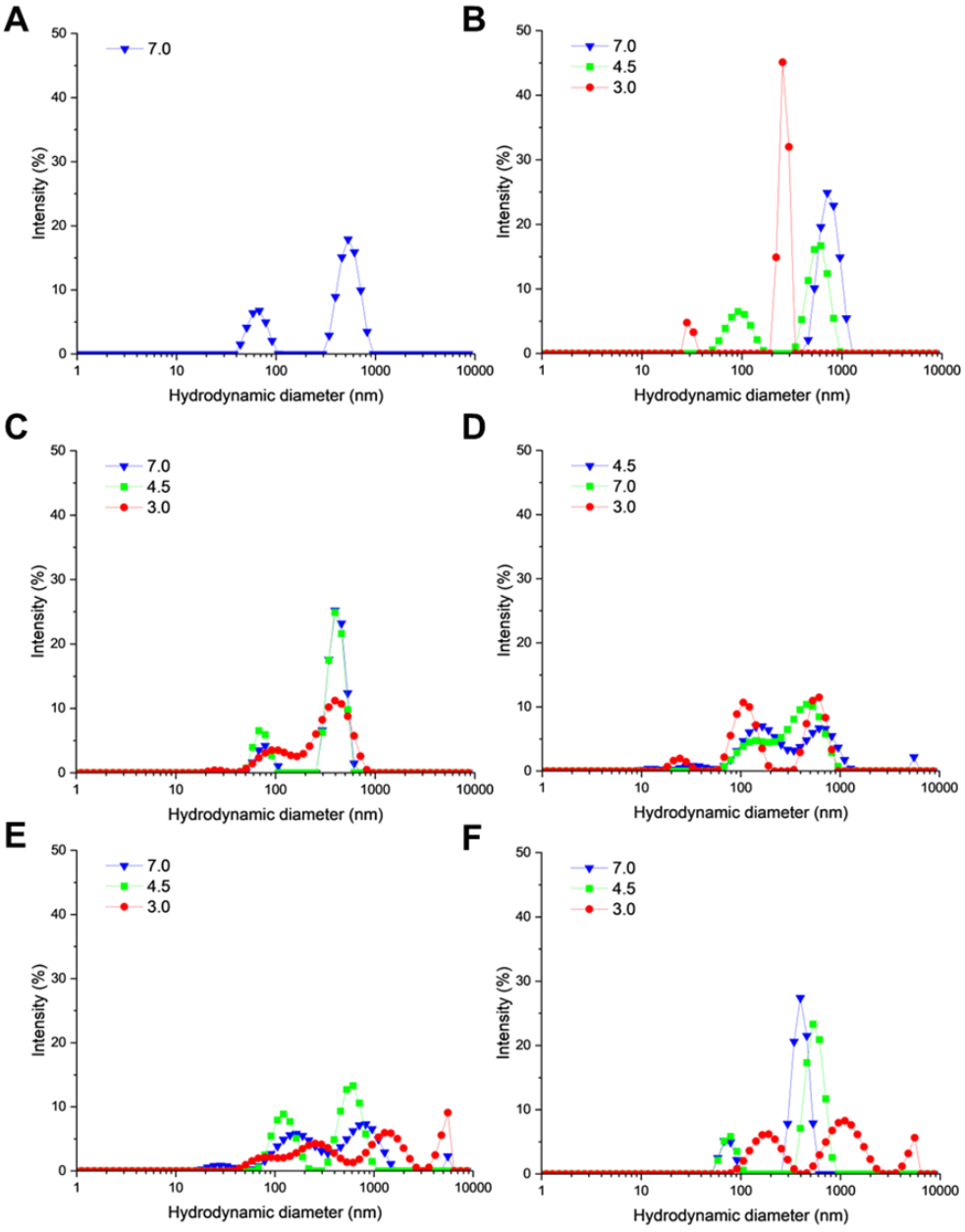

Figure 3.8. Particle size distributions at pH 7.0, 4.5 and 3.0 for sodium caseinate (pH 7.0 only; A), propylene glycol alginate (B), and their mixture (1:1, w:w) after reaction for 2 h at pH 11.0 and 10 mM KCl (C), KH_2PO_4 (D), NaCl (E) or NaH_2PO_4 (F), followed by pH shifting to 7.0 and centrifugation at 5000 *g* for 10 min to take the supernatant for dialysis and analysis.

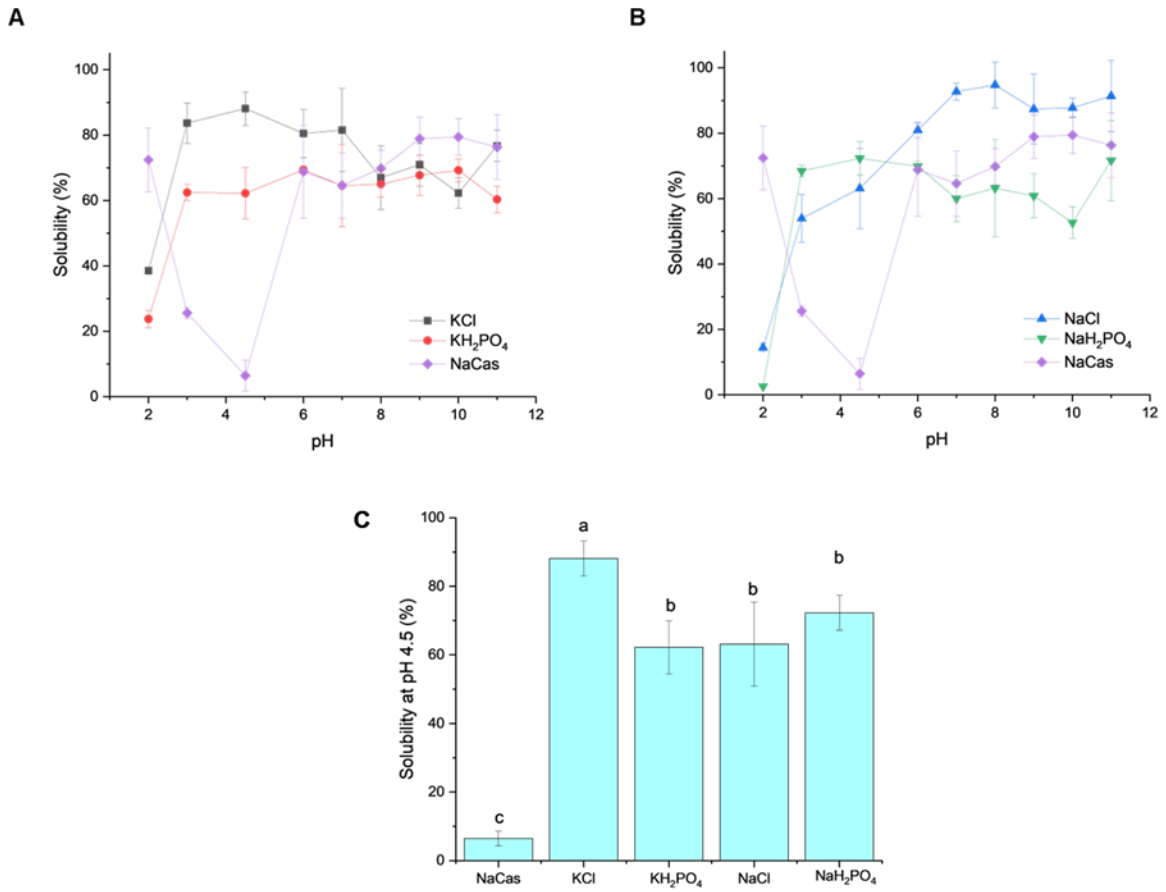

Figure 3.9. Solubility of sodium caseinate (NaCas) and its equal mass mixture with propylene glycol alginate after reaction for 2 h at pH 11.0 and 10 mM of different salts, followed by pH shifting to 7.0 and centrifugation at 5000 *g* for 10 min to take the supernatant for dialysis and analysis: at pH 2.0-11.0 for the KCl and KH_2PO_4 treatments (A), at pH 2.0-11.0 for the NaCl and NaH_2PO_4 treatments (B), and at pH 4.5 for all treatments (C). SDs are shown in error bars (n = 3). Same lowercase and uppercase letters above the bars in C and D stand for significance differences ($p < 0.05$) between treatments with the same concentration of different salts and the same salt at different concentrations, respectively.

Table 2.1. Amino acid composition of casein variants (Chen et al., 2024).

Amino acid	α_{s1}	α_{s2}	β	κ
Ala	8	8	5	14
Arg	6	6	4	5
Asn	14	14	5	8
Asp	4	4	4	4
Cys	2	2	0	2
Gln	16	16	20	15
Glu	24	24	19	12
Gly	2	2	5	2
His	3	3	5	3
Ile	11	11	10	12
Leu	13	13	22	8
Lys	24	24	11	9
Met	4	4	6	2
Phe	6	6	9	4
Pro	10	10	35	20
Ser	17	17	16	13
Thr	15	15	9	15
Trp	2	2	1	1
Tyr	12	12	4	9
Val	14	14	19	11

Table 3.1. ^{23}Na NMR analysis of sodium caseinate (NaCas) treated at different NaCl concentrations and NaCas-propylene glycol alginate conjugate produced at 10 mM NaCl.

Biopolymer	NaCl (mM)	Chemical shift (ppm)	Intensity (a.u.)	Width (Hz)	Area (a.u.)
NaCas	0	-1.08	-5.5	382.59	5889.99
NaCas	10	-11.46	42.3	287.98	34083.71
NaCas	25	-11.81	42.0	287.98	33843.12
NaCas	50	-15.68	37.5	287.98	30215.02
Conjugate	10	-21.44	28.6	287.98	23030.08

Table 3.2. Protein content, moisture content, mass yield, and protein yield of freeze-dried sodium caseinate (NaCas)-propylene glycol alginate (PGA) conjugate powders produced in 10 mM of different salts and NaCas:PGA mass ratios of 1:1 and 1:2 at pH 11.0 and 23 ºC for 2 h.*

Salt	NaCas:PGA	Protein Content (mg/g)	Moisture content (%, wet basis)	Mass Yield (%)	Protein Yield (%)
None**	1:0	853.03 ± 1.09^{a}	2.87 ± 0.76^{a}	-	-
KCl	1:1	846.23 ± 1.00^{a}	1.33 ± 0.36^{b}	86.20 ± 5.23^{a}	85.51 ± 5.19^{a}
KCl	1:2	823.89 ± 0.34^{b}	1.30 ± 0.36^{b}	82.93 ± 2.54^{a}	80.10 ± 2.46^{a}
KH_2PO_4	1:1	836.85 ± 0.46^{a}	0.96 ± 0.18^{b}	89.00 ± 4.94^{a}	87.31 ± 4.86^{a}
KH_2PO_4	1:2	819.59 ± 0.31^{b}	0.98 ± 0.18^{b}	76.67 ± 2.82^{b}	73.66 ± 2.71^{b}
NaCl	1:1	803.30 ± 0.35^{a}	0.60 ± 0.19^{c}	67.80 ± 5.93^{bc}	63.85 ± 5.59^{c}
NaCl	1:2	782.80 ± 1.51^{b}	0.79 ± 0.19^{d}	56.80 ± 5.90^{cd}	52.12 ± 5.45^{d}
NaH_2PO_4	1:1	837.11 ± 0.92^{a}	0.98 ± 0.18^{b}	86.13 ± 6.50^{a}	84.53 ± 6.38^{a}
NaH_2PO_4	1:2	798.87 ± 2.71^{b}	1.18 ± 0.20^{b}	72.00 ± 2.82^{bc}	67.42 ± 2.64^{c}

*Numbers are mean ± SD (n = 3). Different superscript letters represent significant differences among mean values in the same column ($p < 0.05$).

**The NaCas powder without processing.

VITA

Bryan Alberto Castellanos Paez was born and raised in Bogotá, Colombia. Growing up in a vibrant and huge city and within a large family, I was one of six siblings, with four brothers and one sister. From an early age, I displayed a curiosity for science, leading to a deep interest in chemistry, physics, and engineering. This passion drove me to pursue a degree in Chemical Engineering, where I dedicated years to learning the principles of chemical processes, transport phenomena, simulation of chemical reactions, product design, polymers, and materials, along with their applications. Throughout my academic career, I engaged in various research projects and hands-on experiences that strengthened my expertise and technical skills. I am particularly interested in the fields of biopolymers, thermodynamics, chemical reaction, and analytical chemistry, and have aimed to apply this knowledge to areas with potential for impactful, sustainable solutions. I look forward to continuing a career where I can contribute to advancements in chemical, food, pharmaceutical, and supplement industries, with commitment to innovation, sustainability, and environmental stewardship.